

# Supramolecular Chirons Based on Enantiodifferentiating Self-Assembly between Amines and Alcohols (Supraminols)

Stephen Hanessian,\* Raffaele Saladino, Roberto Margarita, and Michel Simard<sup>[a]</sup>

*Dedicated to Professor Jean-Marie Lehn on the occasion of his 60th birthday*

**Abstract:** Homochiral pairs of vicinal diamines and vicinal diols form well-defined crystalline supramolecular assemblies (supraminols) as a result of mutual recognition. X-ray crystallographic analysis shows extensive hydrogen bonding between amine and alcohol groups that results in a hydrophilic inner core and hydrophobic outer peripheral units. The inner core consists of partially or fully hydrogen-bonded amine–alcohol interactions that lead to a pleated-

sheet- or ribbonlike secondary structure. The outer periphery consists of left- or right-handed helical strands of alternating diamine–diol units, depending on the sense of chirality of the diamine and the diol. High enantiomeric enrichment

is possible when an enantiopure diamine and a racemic diol are allowed to interact resulting in a matched homochiral crystalline adduct. In one instance, the occlusion of a molecule of benzene within the assembly was observed. On the basis of competition experiments, some predictions can be made regarding the best matched pairs of diamines and diols, which we have termed *supramolecular chirons*.

**Keywords:** chirality • helical structures • hydrogen bonds • molecular recognition • supramolecular chemistry • supraminols

## Introduction

Supramolecular chemistry<sup>[1]</sup> has evolved into one of the more exciting and thought-provoking subdisciplines of science with far-reaching applications. Lehn's scholarly contributions<sup>[2]</sup> in this area have paved the way to numerous extensions of the original concepts, resulting in the creation of a variety of organized molecular frameworks.<sup>[3]</sup> When such supermolecules are solids, the prospect of discovering interesting physical properties with possible applications in materials science is a sought-after objective and a meeting ground for different technologies.

Advances in self-assembly of organic molecules in particular and the generation of supramolecular structures based on noncovalent interactions have heightened interest in crystal engineering. According to Desiraju,<sup>[4]</sup> crystal engineering is the understanding of intermolecular interactions in the context of crystal packing and in the utilization of such understanding in the design of new solids with desired physical and chemical properties. Aspects of crystal engineering have also been discussed in terms of design, strategy, and

architecture.<sup>[4, 5]</sup> In spite of many contributions in this area, the issue of predicting structural features from the chemical composition and functional properties remains an interesting, challenging, and elusive aim.<sup>[2, 6]</sup> Contrary to normal disconnective analysis in synthesis planning, where a molecular entity such as a natural product is simplified into its basic building blocks<sup>[7]</sup> and then chemically assembled in the forward sense, the organization of molecules of known structure into specific patterns and shapes in the solid state is not predictable. In most cases, thermodynamic forces will ultimately decide the architecture, organization, dimensionality, and, in human terms, the aesthetic quality of the resulting motif.<sup>[8]</sup>

Hydrogen bonding has been an important feature in the noncovalent assembly of neutral molecules possessing donor–acceptor functionalities.<sup>[9]</sup> In this context, Nature has been a most generous provider of examples of hydrogen-bonded entities with nucleic acids, and proteins as marquee supermolecules.<sup>[10]</sup> Hydrogen bonding between neutral amide-type NH and carbonyl-type O atoms has featured prominently in the design and self-assembly of a number of supramolecular structures involving mainly achiral donor–acceptor molecules.<sup>[11]</sup>

The interaction between simple amines and alcohols has been previously demonstrated spectroscopically<sup>[12]</sup> by X-ray diffraction techniques,<sup>[13]</sup> and indirectly based on analytical techniques associated with HPLC.<sup>[14]</sup> In a recent elegant study, Ermer and Eling<sup>[15]</sup> reported on the self-assembly of diphe-

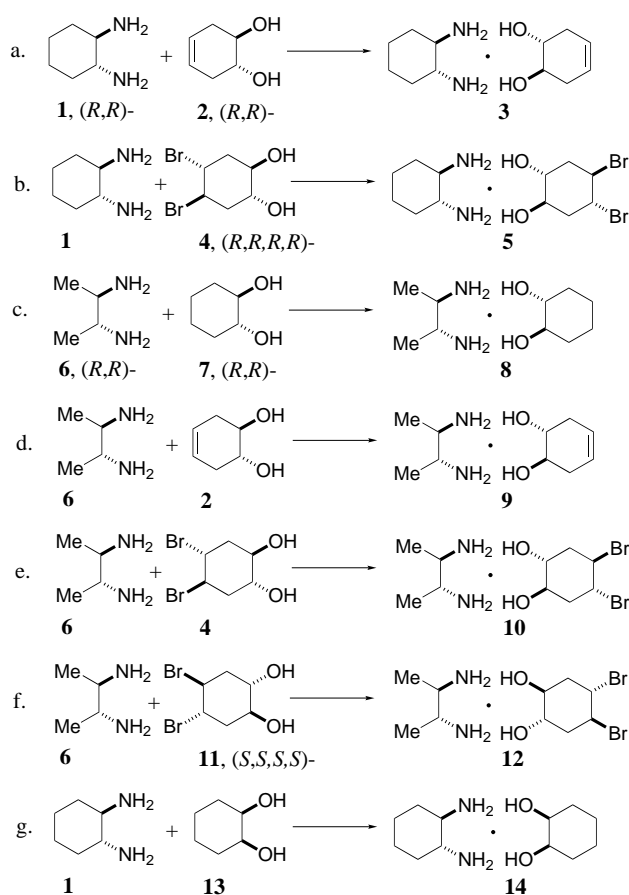
[a] Prof. Dr. S. Hanessian, R. Saladino, R. Margarita, M. Simard  
Department of Chemistry, Université de Montréal  
C.P. 6128, Succursale Centre-ville, Montréal,  
Québec H3C3J7 (Canada)  
Fax: (+1)514-343-5728  
E-mail: hanessia@ere.umontreal.ca

nol–diamine molecules into supramolecular arrays. Our concurrent studies<sup>[16]</sup> showed for the first time that chiral nonracemic pairs of vicinal diamines and diols could self-assemble to give crystalline three-dimensional helical motifs (*supraminols*). Furthermore, the sense of helicity was dependent on the chirality of the partners. Although (*R,R*)- or (*S,S*)-1,2-diaminocyclohexane exists as a layered two-dimensional structure in the solid state, it behaves as a matrix to accommodate a matching diol partner, a fact which leads to a right- or left-handed three-dimensional helical superstructure.<sup>[16]</sup>

The core of these assemblies consists of hydrogen-bonded pleated sheets or ribbons depending on the nature of the  $C_2$ -symmetrical diol. It was therefore of interest to delineate structural features in the diamine and diol units that favor a pleated-sheet- or a ribbonlike hydrogen-bonding pattern in the core of the corresponding three-dimensional assembly. The notion of *supramolecular chirons* is introduced to identify basic units that are the chiral counterparts of supramolecular synthons.<sup>[4]</sup> We thus define a *supramolecular chiron* as the minimal homo- or heterochiral molecular unit or ensemble capable of generating ordered superstructures by self-assembly through hydrogen-bonding or other noncovalent forces, and leading to topologically distinct enantio- or diastereopure architectures. Issues related to chirality in the context of supramolecular chemistry have not been addressed in a systematic manner.<sup>[17]</sup>

## Results

When a suspension containing equimolar amounts of enantiomerically pure (*R,R*)-1,2-diaminocyclohexane (**1**)<sup>[18]</sup> and (*R,R*)-4-cyclohexene-1,2-diol (**2**)<sup>[19]</sup> in benzene was brought to the reflux temperature of the solvent and the clear solution formed was allowed to cool, a crystalline product was formed in over 90% yield (Scheme 1). The same procedure for (*1R,2R,4R,5R*)-4,5-dibromocyclohexan-1,2-diol (**4**)<sup>[19]</sup> and diamine **1** gave a crystalline adduct **5**. Spectroscopic and X-ray crystal structure analysis of adducts **3** and **5** showed the formation of a 1:1 complex consisting of one molecule each of diamine and diol, and linked by a pair of interactions well within the distance of a definite hydrogen bond. Table 1 contains pertinent crystallographic data for the *supraminols* discussed in this paper.<sup>[20]</sup> The same procedure failed to afford solid adducts when **1** was mixed with enantiomerically pure (*R,R*)-1,2-cyclopentanediol, (*1R,2R*)-3,5-cyclohexadiene-1,2-diol, (*1S,2S*)-4-cyclohexene-1,2-diol, or (*1S,2S,4S,5S*)-4,5-dibromocyclohexan-1,2-diol. Adducts **3** and **5** form well-defined and well-ordered supramolecular structures that self-assemble through a unique network of hydrogen bonds. In the adduct **3**, cyclohexane and cyclohexene moieties are stacked in four columns (Figure 1, panels A, B). The hydrogen-bonded motif of the core has the shape of a right-handed helical ribbon similar to that previously observed for the crystalline adduct between enantiomerically pure (*R,R*)-1,2-diaminocyclohexane and (*R,R*)-2,3-butanediol,<sup>[16]</sup> and different from the pleated-sheet-like motif found in the adduct of **1** and (*R,R*)-cyclohexane-1,2-diol.<sup>[16]</sup> Thus, the presence of the



Scheme 1. Vicinal diamines and diols comprising carbocyclic and acyclic structures and their adducts.

4,5-double bond in the cyclohexene ring of the diol partner **2** markedly influences the topology of the hydrogen-bonded motif of the core. The helical ribbon-shaped core consists of eight-membered square planar hydrogen-bonded units in which one of the  $\text{NH}\cdots(\text{O})$  hydrogen bonds is weak (with average long and short distances of 2.56 Å and 2.24 Å) (Figure 1, panels C, D). Nitrogen and oxygen atoms act as donors or acceptors leading to a fully hydrogen-bonded network in the core. Pairs of diamine and diol units are interlinked by three antidromic hydrogen-bonded strands that run parallel at a distance of 6.728 Å. The hydrogen-bonding pattern in the helical strand utilizes the amino group as donor and hydroxyl group oxygen as acceptor generating a left-handed helical strand with a pitch of 20.184 Å (Figure 1, panel E). A remarkable consequence is the emergence of unusual topological features in the superstructure. Thus, while the peripheral residues consisting of diamine and diol units adopt a left-handed helical shape, the ribbonlike hydrogen-bonded motif within the core has an opposite helicity (Figure 1, panels D and E). A stereoview of the hydrogen-bonding network along the *a* axis can be seen in Figure 1F. A CPK representation of the helical structure of **3** is shown in Figure 2.

In the adduct **5**, the cyclohexane moieties of the diamine and of the diol are stacked in four columns similarly to the adduct **3**. In the case of **5**, however, the diol exists in two different orientations, rotated by  $\sim 20^\circ$  in the *a*–*c* plane of the

Table 1. Crystallographic data collection and structure refinement information.

	<b>3</b>	<b>5</b>	<b>8</b>	<b>9</b>	<b>10</b>	<b>12</b>	<b>14</b>
space group	$P2_12_12_1$	$P2_1$	$C2$	$C2$	$P2_12_12_1$	$P2_12_12_1$	$C2$
$Z$	4	2	4	4	4	2	8
cell constants							
$a$ [Å]	6.7282(18)	11.056(6)	18.563(7)	18.547(6)	6.432(2)	7.725(2)	20.792(6)
$b$ [Å]	10.697(4)	6.507(5)	6.7360(12)	6.779(3)	12.113(6)	7.924(2)	11.516(3)
$c$ [Å]	19.828(7)	11.599(6)	13.155(3)	12.660(6)	18.496(7)	11.540(3)	15.747(5)
$\beta$ [°]	90.0	97.78(4)	126.54(2)	109.14(3)	90.0	90.0	133.18(2)
$V$ [Å <sup>3</sup> ]	1427.1(8)	826.8(9)	1321.6(6)	1503.8(11)	1441.0(10)	706.4(3)	2749.5(14)
$\mu$ [mm <sup>-1</sup> ]	0.57	6.20	0.57	0.57	7.07	7.21	0.60
$\rho_{\text{calcd}}$ [g cm <sup>-3</sup> ]	1.063	1.559	1.027	1.066	1.669	1.702	1.113
$F(000)$	504	392	456	532	728	364	1024
radiation	Cu <sub>K<math>\alpha</math>1</sub>	Cu <sub>K<math>\alpha</math>1</sub>	Cu <sub>K<math>\alpha</math>1</sub>	Cu <sub>K<math>\alpha</math>1</sub>	Cu <sub>K<math>\alpha</math>1</sub>	Cu <sub>K<math>\alpha</math>1</sub>	Cu <sub>K<math>\alpha</math>1</sub>
$\theta_{\text{max}}$ [°]	70.0	70.0	70.0	70.0	70.0	70.0	70.0
scan mode	$\omega/2\theta$	$\omega/2\theta$	$\omega/2\theta$	$\omega/2\theta$	$\omega/2\theta$	$\omega/2\theta$	$\omega/2\theta$
$h, k, l$ ranges	$\pm 8, +13, +24$	$\pm 12, \pm 7, +14$	$\pm 22, \pm 8, +16$	$\pm 22, \pm 8, +15$	$\pm 7, +14, +22$	$\pm 9, +9, +14$	$\pm 25, \pm 14, +19$
no. of reflns measured	10042	4034	4892	5615	9403	4715	10136
no. of unique reflns	2705	2043	2471	2825	2734	1348	5114
$R_{\text{merge}}$	0.033	0.082	0.039	0.065	0.130	0.147	0.045
no. with $I > 2.00\sigma(I)$	2456	1475	2383	2225	2316	1066	4761
no. of parameters	242	258	224	159	150	76	298
$R1$ (obs. ref. only) <sup>[a]</sup>	0.040	0.061	0.038	0.075	0.062	0.054	0.051
$wR2$ (all data) <sup>[b]</sup>	0.104	0.160	0.113	0.198	0.188	0.135	0.148
$S$ <sup>[c]</sup>	1.00	0.98	1.11	0.99	1.06	0.97	1.09

[a]  $R1 = \Sigma(|F_o| - |F_c|) / \Sigma(|F_o|)$ . [b]  $wR2 = [\Sigma[w(F_o^2 - F_c^2)^2] / \Sigma[w(F_o^2)^2]]^{1/2}$ . [c]  $S = [\Sigma[w(F_o^2 - F_c^2)^2] / (\text{No. of reflns} - \text{No. of params.})]^{1/2}$

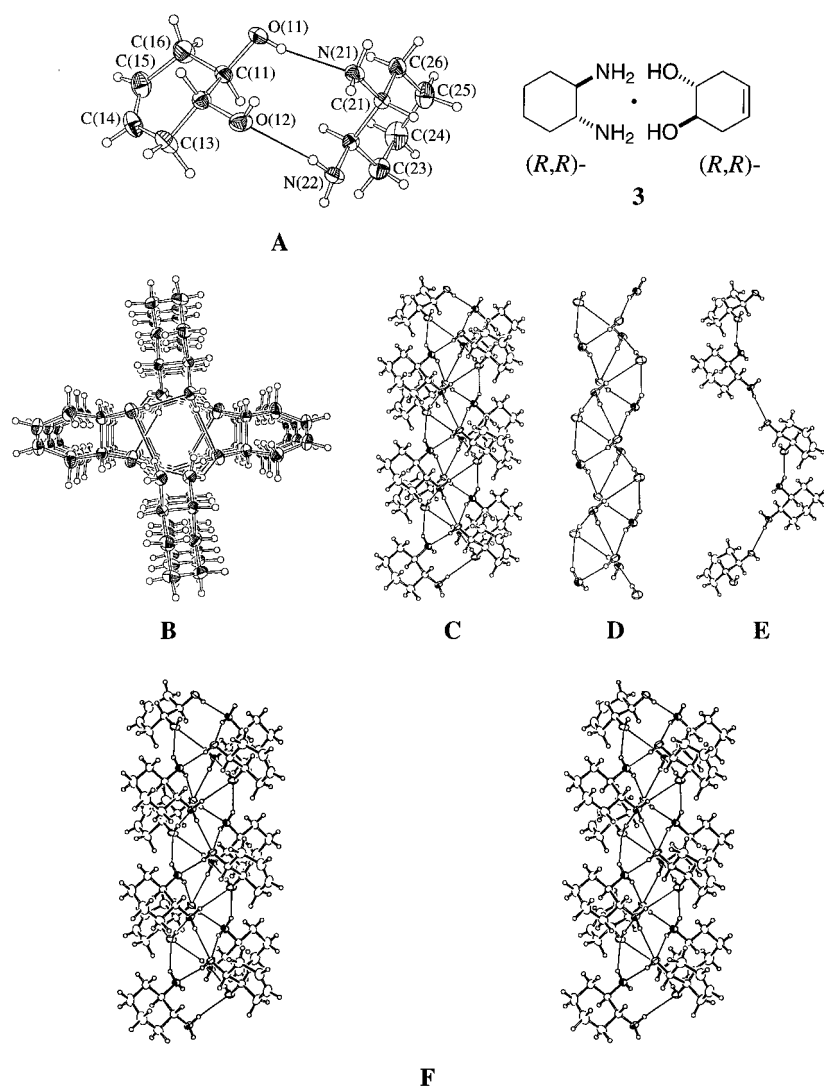


Figure 1. A) ORTEP view of the molecular adduct **3** (H-bonds are represented by thin lines); B) H-bonding network of adduct **3** (top view down the  $a$  axis); C) side view of the H-bonding network (H-bonds are represented by thin lines) showing the full coordination of all heteroatoms; D) simplified representation of the view in (C) showing the right-handed helical motif constituting the ribbonlike H-bonded core of the assembly; E) single strand for H-bonded units extracted from the triple-stranded helicate structure in **3** showing left-handed helicity. H-bonds are uniformly established between  $\text{NH}_2$  donors and OH acceptors of alternate diamine and diol molecules; F) stereoview of the H-bonding network (side view along the  $a$  axis).

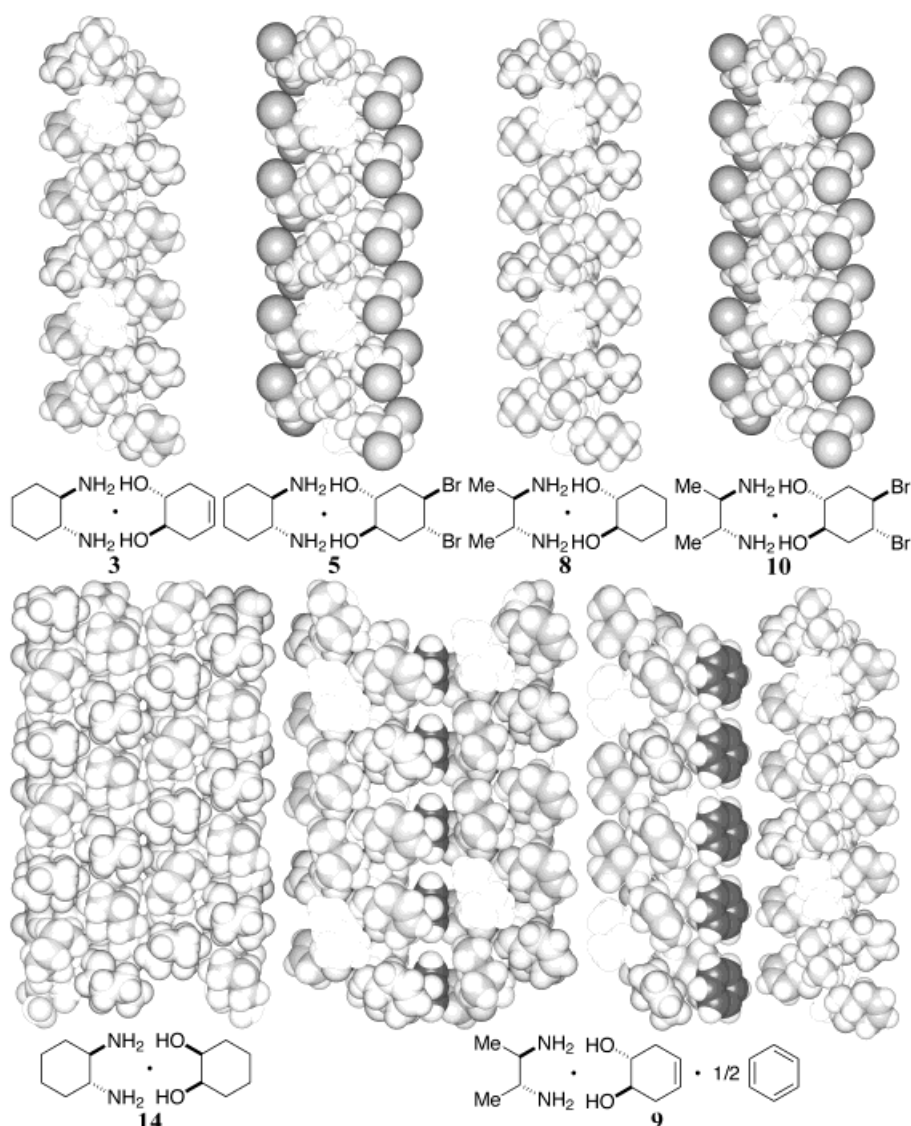


Figure 2. CPK representation of the helical secondary structure of **3**, **5**, **8**, **10**, **9**. Diamine residues are shown in blue and diols in red within one strand of the helicates in **3**, **5**, **8**, **9**, and **10**. Bromine atoms are shown in green. For **14**, a segment showing two contiguous elements of the layered structure is depicted with diol in red and diamine in gray. For **9**, benzene molecules included in the triple-stranded helical crystal structure are shown with black carbon atoms; CPK of **9** with partially rotated left-hand motif with included benzene molecules and an artificial separation of the right-hand motif (not rotated).

adduct. For the sake of clarity, only the ORTEP views of the molecular structure for the complex formed from the major diol component are shown in Figure 3 (panels A and B). An explanation of the occurrence of two different diol motifs could be found in the presence of two strong van der Waals interactions (2.13 Å for the bromine–hydrogen interaction and 3.09 Å for the bromine–carbon interaction) between adjacent columns in the superstructure. While a ribbonlike hydrogen-bonded core is evident, only one of the two amino groups is fully engaged in hydrogen bonding, as depicted in Figure 3 (panels C and D). Three antidiromic hydrogen-bonded strands run parallel at a distance of 6.507 Å, generating a left-handed helical strand with a pitch of 19.521 Å (Figure 3, panels C, D, and F). A CPK representation of the helical structure of **5** is shown in Figure 2.

In an attempt to extend our knowledge about the relationships between structure and hydrogen-bonding capabilities for the supraminols, we utilized (*R,R*)-2,3-diaminobutane (**6**)<sup>[22]</sup> as a new diamine component. Equimolar amounts of **6** and enantiomerically pure (*R,R*)-cyclohexane-1,2-diol (**7**) afforded a crystalline adduct **8**. Familiar stacking of butane and cyclohexane units can be seen as in the case of **3** (Figure 4, panels A and B). Similarly, the fully hydrogen-bonded core consists of a right-handed helical ribbon (Figure 4, panels C, D, and F). The OH⋯(N) hydrogen bonding (average 1.97 Å) and the NH⋯(O) hydrogen bonding values (average long bond 2.44 Å, short bond 2.23 Å) are smaller than those observed for **3**. Three antidiromic hydrogen-bonded strands run parallel at a distance of 6.799 Å, generating a left-handed helical strand with a pitch of 20.337 Å (Figure 4, panels D and E). This helix is more compressed in the *a*–*c* plane and more extended along the *b* plane compared with that of (*R,R*)-1,2-diaminocyclohexane and (*R,R*)-2,3-butanediol.<sup>[16]</sup> A CPK representation of the helical structure of **8** is shown in Figure 2.

The adduct between (*R,R*)-4-cyclohexen-1,2-diol (**2**) and (*R,R*)-2,3-diaminobutane (**6**) afforded a crystalline solid **9** (Scheme 1). The overall topology of **9** was similar to that of **8** (Figure 5, panels A and E). However, benzene molecules were included in the crystal structure of **9**, and located at the intersection of four columns in a plane parallel to the *a*–*b* plane of the unit cell of the adduct.<sup>[22]</sup> No stacking interactions could be observed between the benzene ring and the double bond of the diol (Figure 5, panels F, B). Each benzene unit exhibits a hydrogen–hydrogen van der Waals interaction (2.81 Å) with the next benzene unit along the *b* axis. Interestingly, the preparation of **9** in a 1:1 mixture of benzene and toluene afforded only crystals that included benzene. Some noteworthy structural features are evident from the comparison of the adducts **9** and **3**. In **9** the OH⋯(N) hydrogen-bonding distances (average 1.94 Å) and NH⋯(O) (average long bond 2.42, short bond 2.24 Å) are smaller than those in **3**. The

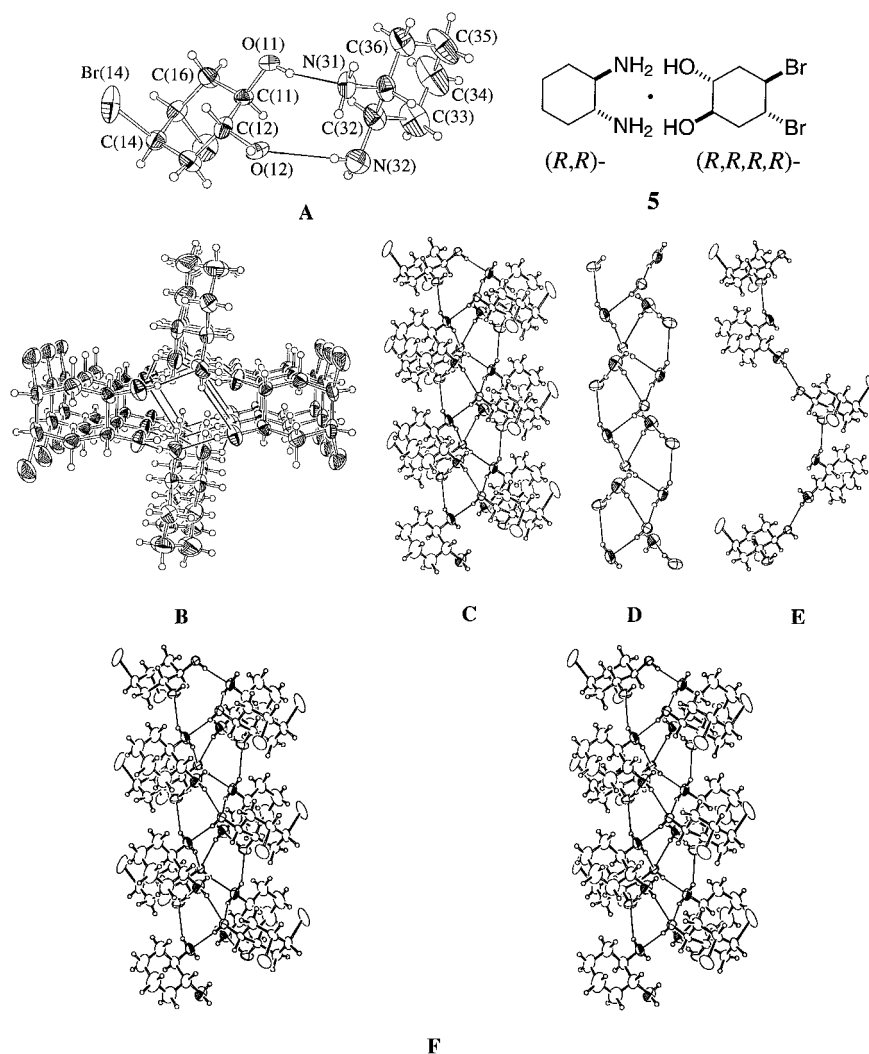
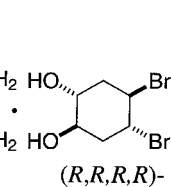


Figure 3. A) ORTEP view of the molecular adduct **5** (H-bonds are represented by thin lines); B) H-bonding network of adduct **5** (top view down the *a* axis); C) side view of the H-bonding network (H-bonds are represented by thin lines) showing the coordinations of oxygen atoms and the full coordination of nitrogen atoms; D) simplified representation of the view in (C) showing the left-handed helical motif constituting the ribbonlike H-bonded core of the assembly; E) single strand for H-bonded units extracted from the triple stranded helicate structure in **5** showing left-handed helicity. H-bonds are uniformly established between NH<sub>2</sub> donors and OH acceptors of alternate diamine and diol molecules; F) stereoview of the H-bonding network (side view along the *b* axis).

helical structure of **9** is compressed along the *a*–*c* plane and more extended along the *b* axis, probably because this geometry is necessary to accommodate the included benzene molecules (Figure 5, panels C, D, E, and F). A CPK representation of the helical structure of **9** with the included benzene molecules is shown in Figure 2.

Both enantiomers of 4,5-dibromocyclohexan-1,2-diol<sup>[19]</sup> afforded crystalline adducts **10** and **12** with the diamine **6** (Scheme 1). In the case of **10**, the cyclohexane rings of both molecules are aligned into four vertical columns with the polar groups facing inward as expected (Figure 6, panels A and B). The hydrogen-bonding motif of the core is an incomplete right-handed helical ribbon (Figure 6, panels C, D). One of the NH $\cdots$ (O) hydrogen bonds is very weak (2.54 Å). The corresponding NH $\cdots$ (O) angle value of 132° deviates from the theoretical value, hence the absence of the



**5**

full hydrogen bonding seen in the structures of **3** or **9**. Three antidromic hydrogen-bonded strands run parallel at a distance of 6.432 Å, generating a helical strand with a 19.30 Å pitch that is somewhat compressed along the *a*–*c* plane compared to all other helicates in this series of supraminols (Figure 6, panels D, E, and F). This unexpected structural feature could be due to the steric encumbrance of the axial bromine atoms. Moreover, there are no van der Waals interactions for either bromine–bromine or bromine–hydrogen atoms.<sup>[23]</sup> The lowest value for the bromine–bromine contact is 4.576 Å and that for the bromine–hydrogen is 3.27 Å. A CPK representation of the helical structure of **10** is shown in Figure 2.

Unlike **10**, the adduct **12** consists of a vastly interlinked bidirectional hydrogen-bonded network as the constitutional element of the assemblage (Figure 7). Channels run inside the core along the *b* axis (Figure 7, panels B, C, E) reminiscent of the crystal structure previously observed for the adduct formed from enantiomerically pure (*R,R*)-1,2-diaminocyclohexane and (*R,R*)-tartaric acid.<sup>[16, 24]</sup> The supraminol structure **12** exhibits a strong face-to-face interaction between the bromine atoms along the *b* axis of the adduct. The interresidue

bromine–bromine atoms distance was 3.38 Å, which might be responsible for deviations from the anticipated helical structure observed for the matched pair in **10**. The network develops in a plane perpendicular to the *c* axis (Figure 7, panel D). Very weak OH $\cdots$ (N) hydrogen bonds are present along the *a*–*b* plane (2.54 and 2.92 Å) and the corresponding angle values of 167° and 138° deviate from the theoretical values.

At this juncture, it is informative to recall that all the crystalline adducts studied so far have consisted of C<sub>2</sub>-symmetrical vicinal diamines and diols comprising carbocyclic and acyclic structures (Scheme 1, entries a–f). To study the effect of chirality in diol partners we looked at the adducts formed from (*R,R*)-1,2-diaminocyclohexane (**1**) and *cis*-1,2-cyclohexanediol (**13**). The crystalline adduct **14** has a three-dimensional structure that is self-assembled in a two-direc-

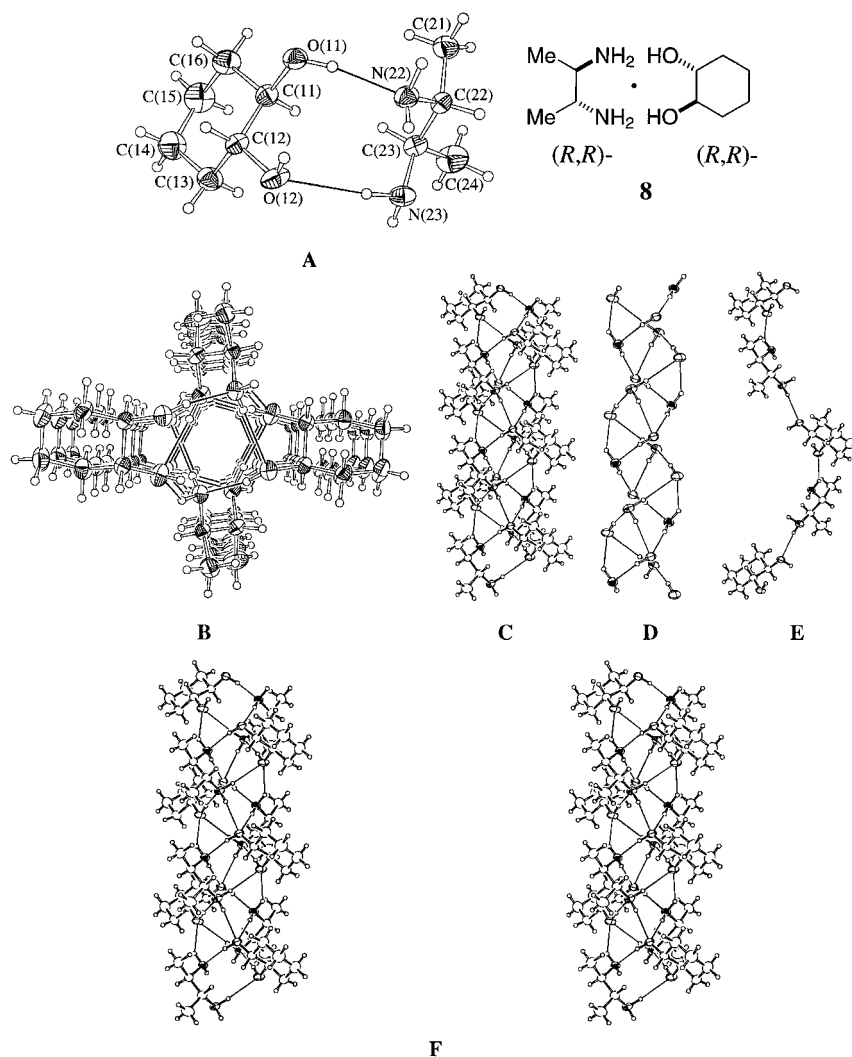


Figure 4. A) ORTEP view of the molecular adduct **8** (H-bonds are represented by thin lines); B) H-bonding network of adduct **8** (top view down the *a* axis); C) side view of the H-bonding network (H-bonds are represented by thin lines) showing the full coordination of all heteroatoms; D) simplified representation of the view in (C) showing the right-handed helical motif of the ribbonlike H-bonded core of the assembly; E) single strand for H-bonded units extracted from the triple stranded helicate structure in **3** showing left-handed helicity. H-bonds are uniformly established between  $\text{NH}_2$  donors and OH acceptors of alternate diamine and diol molecules; F) stereoview of the H-bonding network (side view along the *b* axis).

tional hydrogen-bonding network. Although the nature of the interactions involved is markedly different from that of the other adducts discussed in this paper, the top view and the side view of the assembly (Figure 8, panels A, B, D, and E) present a similarity to the previously described charged network for carbonated (*R,R*)-1,2-diaminocyclohexane.<sup>[16]</sup> In contrast to other adducts shown in Scheme 1, where a ratio of 1:1 diol and diamine moiety was involved, the supramolecular chiron in **14** is defined by two diamine and two diol moieties. An incomplete ribbonlike core motif characterizes the adduct, and there are two interlinking hydrogen bonds between O(22)–H(22) and N(32) for any unit cell alternating at 11.516 Å on either side of the ribbon. This results in a layered structure which develops in the second direction (*a* axis), reminiscent of the carbonated (*R,R*)-1,2-diaminocyclohexane assembly.<sup>[16]</sup>

### Competition experiments and enantiomeric resolution:

Some competition experiments were done by adding different alcohols to preformed supraminols in order to evaluate the relative stability of each adduct (Scheme 2). When a suspension containing equimolar amounts of **15** and **16** in benzene was brought to the reflux temperature of the solvent and the clear solution allowed to cool, crystalline **15** was obtained in 89% yield as the only recovered solid adduct. Moreover, when the experiment was repeated under similar conditions with **17**<sup>[16]</sup> in the presence of **7**, again crystalline **15** was recovered in 78% yield as the only solid adduct. These experiments demonstrate that **15** crystallizes preferentially to **17**. As expected, **15** was also obtained as the only adduct when the oily complex **18** was mixed with an equimolar amount of **7**. The tendency of (*R,R*)-diols to replace the (*S,S*)-diols in supraminols assembled from a (*R,R*)-diamine was further confirmed in the exchange study with enantiomeric diol pairs. When a suspension of an equimolar amount of **18** and **16** was heated to the reflux temperature in ben-

zene and the resulting clear solution allowed to cool, crystalline **17** was obtained in 94% yield and 99% *de* (Scheme 2). In a similar way, a competition experiment between **19** and **2** afforded **3** in 83% yield and 98% *de*. The different behavior shown by (*R,R*)- and (*S,S*)-diols in the crystallization with **1** was successfully used for the enantiomeric enrichment of the racemic *trans*-diol **2**. When a sample of **1** was heated in benzene with equimolar amounts of racemic *trans*-diol **2**, a solid containing the (*R,R*)-diol **2** with a diastereomeric enrichment of about 82% crystallized out of solution. Further recrystallization allowed an enrichment up to ca. 98% *de*.<sup>[25]</sup>

Finally, when a suspension of equimolar amounts of **14** and **7** was brought to the reflux temperature of benzene and the clear solution allowed to cool, crystalline **15** was obtained in 86% yield (Scheme 2).

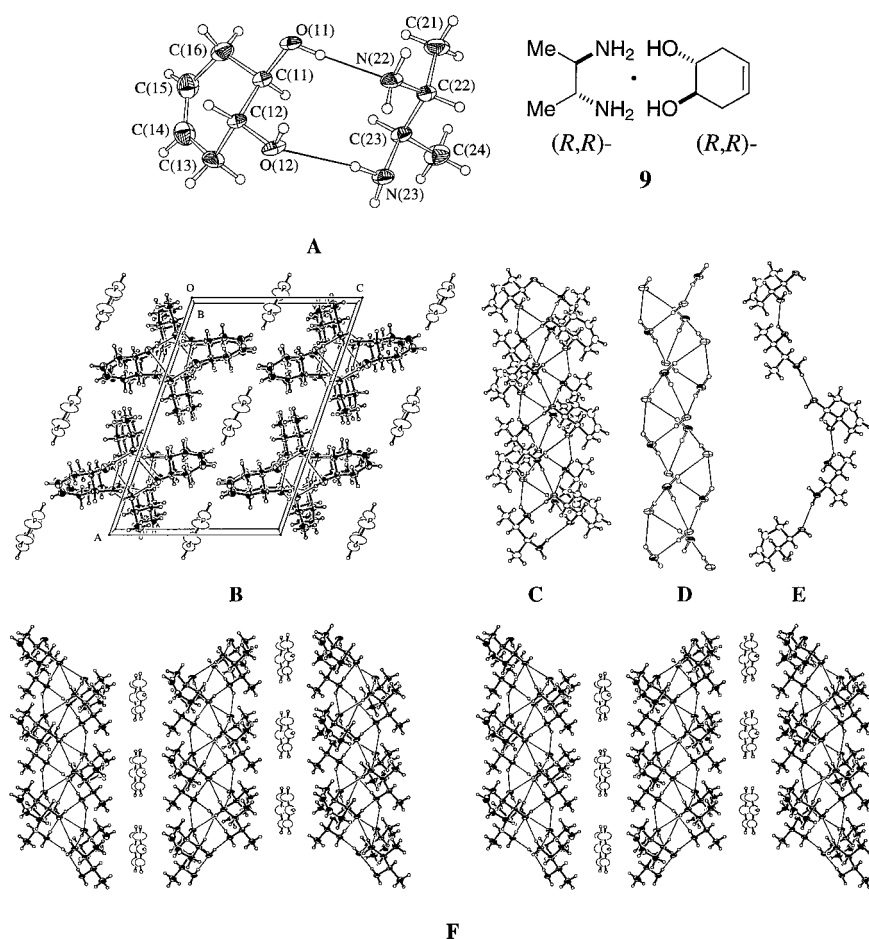


Figure 5. A) ORTEP view of the molecular adduct **9** (H-bonds are represented by thin lines); B) ORTEP view of the inclusion complex between benzene and adduct **9** (top view down the *a* axis, H-bonds are represented by thin lines); C) side view of the H-bonding network (H-bonds are represented by thin lines) showing the full coordination of all heteroatoms; D) simplified representation of the view in (C) showing the right-handed helical motif of the ribbonlike H-bonded core of the assembly; E) single strand for H-bonded units extracted from the triple stranded helicate structure in **9** showing left-handed helicity. H-bonds are uniformly established between  $\text{NH}_2$  donors and OH acceptors of alternate diamine and diol molecules; F) stereoview of the inclusion complex between benzene and adduct **9** showing the spatial proximity between the hydrogens of two consecutive benzene molecules (side view along the *b* axis).

#### Hydrogen-bonded core structure as a function of torsional and dihedral angles:

As shown in Table 2, it is possible to correlate some dihedral angle values of the diol and diamine moieties with the ribbon-shaped versus pleated-sheet-like core motif for helical supraminols. The absolute  $\delta$  value observed for the diol component of adducts with a ribbon-shaped core is in general smaller than that found in the pleated-sheet motif with the exception of **5** and **10**, probably as a result of the presence of the bulky axial bromine atoms. The sign of the  $\delta$  angle depends on the chirality of the diols with a positive value for (*S,S*)-diols and a negative one for (*R,R*)-diols. The absolute  $\delta$  value observed for the diamine component of all the adducts with a ribbon-shaped core is in general also smaller than that found in the pleated-sheet-like motif present in **15** and **15a**.

#### NMR studies in solution:

Interchangeable donor–acceptor interactions between diamines and diols were also manifested in solution as evident

from  $^1\text{H}$  NMR spectroscopy in 0.1M  $[\text{D}_6]$ benzene and  $\text{CDCl}_3$  solutions at  $25^\circ\text{C}$  (Table 3). A downfield shift is observed for both the  $\text{CHOH}$  and the  $\text{CHNH}_2$  protons in all the adducts. In particular, the ribbon-shaped core adducts **3**, **5**, **10** show a higher downfield shift for the  $\text{CHOH}$  signal than that observed for **15**, which is characterized by a pleated-sheet motif, particularly in  $[\text{D}_6]$ benzene (entry 8). The adducts **3** and **5** with ribbon-shaped cores formed between (*R,R*)-1,2-diaminocyclohexane and cyclic alcohols (entries 1 and 2) show a shift for the  $\text{CHOH}$  signal further downfield than that of **17** (entry 9). In a similar way, adducts **3** and **5** show a shift for the  $\text{CHOH}$  signal further downfield than that of all the ribbon-shaped core adducts of the (*R,R*)-1,2-butanediol (entries 4–7). Moreover, in all adducts the individual  $\text{CHOH}$  and  $\text{CHNH}_2$  signals collapse to single broad signals, the position of which changes in proportion to the amount of added diol (as shown by a titration experiment between **1** and **7**). Generally an upfield shift is observed for the  $\text{CHOH}$  signal and a downfield shift for the  $\text{CHNH}_2$  signal of **3** and **5** (entries 1 and 2). An upfield shift is observed for

adducts **9**, **10**, **12**, and **14**, which consist of the (*R,R*)-2,3-diaminobutane and various diols (entries 4–7).

Since a number of adducts did not crystallize or gave crystals that were not suitable for X-ray analysis, we studied their  $^1\text{H}$  and  $^{13}\text{C}$  spectra in order to establish the existence of hydrogen-bonded associations. Scheme 3 depicts the structures of a variety of diamine–diol and diamine–alcohol adducts prepared by mixing equimolar quantities in benzene. Except for the adduct **27**, which afforded fine needles, all the adducts were oils. Characteristic downfield shifts of the  $\text{CHOH}$  and  $\text{CHNH}_2$  signals were observed in their  $^1\text{H}$  NMR spectra of adducts **20–22**; we therefore conclude that combinations of vicinal  $\text{C}_2$ -symmetrical diols were in fact mutually recognized, with the exception of adduct **23**, in which overlapping resonances precluded any deduction. In order to assess the importance of geometry, distance, and symmetry, we studied the solution interactions of diamine–diol and diol–amine pairs as in **24–26** by  $^1\text{H}$  NMR. Although some shifts were observed, they were not as significant as in other better matched adducts (Table 3). The spectrum of **28** did not

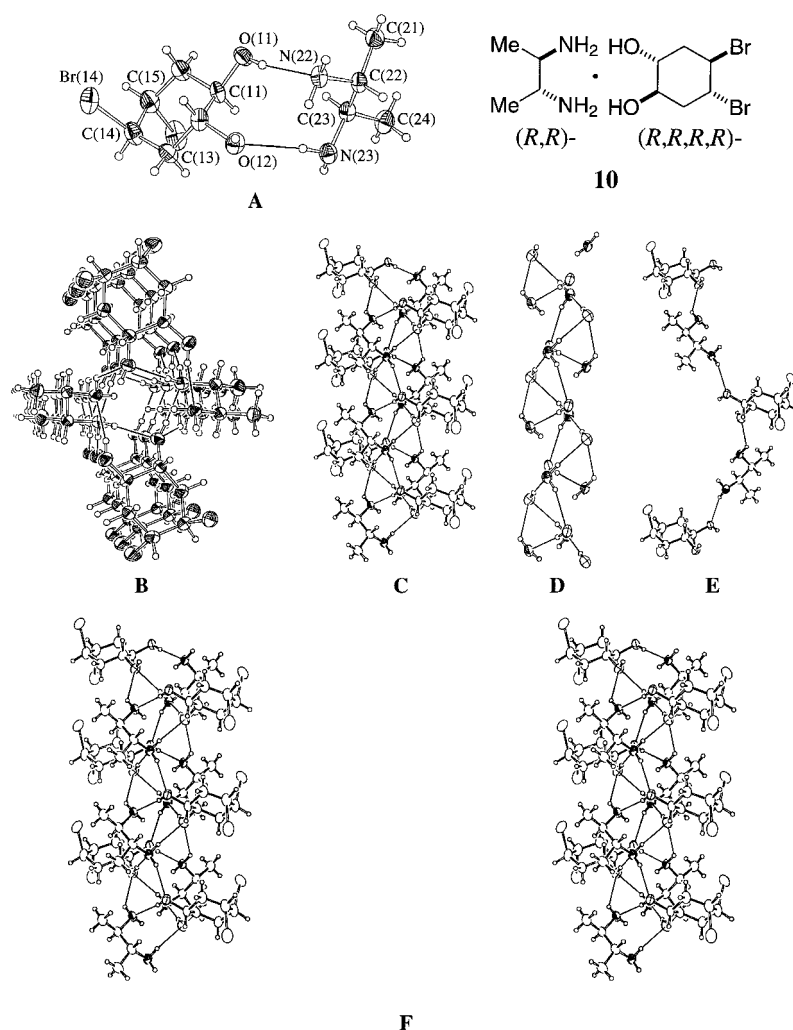


Figure 6. A) ORTEP view of the molecular adduct **10** (H-bonds are represented by thin lines); B) H-bonding network of adduct **10** (top view down the *a* axis); C) side view of the H-bonding network (H-bonds are represented by thin lines) showing the coordination of oxygen and nitrogen atoms; D) simplified representation of the right-handed helical motif of the ribbonlike H-bonded core of the assembly; E) single strand for H-bonded units extracted from the triple stranded helicate structure in **10** showing left-handed helicity. H-bonds are uniformly established between  $\text{NH}_2$  donors and OH acceptors of alternate diamine and diol molecules; F) stereoview of the H-bonding network (side view along the *a* axis).

show any difference in chemical shift for either component, no doubt because of the diminished basicity of the diamine, which could explain the lack of adduct formation.

Molecular recognition was nicely demonstrated for the adducts **22** and **27** as seen in Figure 9. Thus a 1:1 mixture (spectrum C, Figure 9, left) and a 0.5:1 mixture (spectrum D) of **22** clearly shows a resonance for the matched *R,R/R,R*-pair and another for the unbound diol at lower field (presumably, the *S,S*-diol). Likewise, a 1:1 mixture of racemic 1,2-diaminocyclohexane and (*R*)-binaphthol (Figure 9, right) could be easily distinguished from an adduct containing 35% enantioenriched diamine and an adduct of two enantiopure components (spectra B, C, D). Thus, given the requisite geometry and the basicity/acidity characteristics between pairs of diamines and diols, NMR spectroscopy can be a valuable tool to establish the existence of molecular recognition in the absence of crystal structure data.

## Discussion

We have reported the preparation and X-ray single-crystal structural studies of several new uncharged metal-free supramolecular assemblies that result from the association of vicinal  $C_2$ -symmetrical (Scheme 1) diamines and diols. Alternating units of (*R,R*)-diamines and (*R,R*)-diols are interlinked by hydrogen bonds between one amino and one alcohol group to give rise to single strands. A full turn of the helix will encompass two pairs of diamines and diols. In the homochiral (*R,R*)-series, the inner core consists of a right-handed ribbon-shaped hydrogen-bonded array that can be fully or partially associated. The column-shaped supramolecules are organized so that one amino and one hydroxyl group are part of the inner, extensively hydrogen-bonded core, while the other pair is involved in an outer peripheral hydrogen-bonded interaction that links the hydrophobic backbone of the diamine and diol units. A fascinating feature observed in our previous study of supramolecules<sup>[16]</sup> was the change in the sense of helicity of the strands, from left-handed to right-handed, caused simply by changing the chirality of the diamine or diol partner (compound **1** and **7**,

compared with **1** and enantiomer of **7** (Table 2 **15** and **15a**, respectively). It is of interest and somewhat intriguing that the adducts **10** and **12** formed from the same diamine **6** and the all-*R* dibromide **4** or all-*S* enantiomer **11** exhibit different molecular networks (helix versus bidirectional layers). Another fascinating feature that distinguishes seemingly identical adduct structures such as **3** and **15** (Schemes 1 and 2) is the ribbon-shaped hydrogen-bonded core in the former, and a pleated-sheet-like hydrogen-bonded core in the latter. Figure 10 depicts the hydrogen-bonded inner-core motifs for a number of supramolecules. The ribbon-shaped hydrogen-bonded motif is clearly evident in the case of **3**, **5**, **10** and **17**. However, complete hydrogen bonding is observed in only the inner core of **3** and **17**. The hydrogen bonding seen in **5** and **10**, while sufficient to maintain the ribbon-shaped motif, is only partial, perhaps as a result of the geometric constraints imposed by the presence of the bulky bromine atoms<sup>[23]</sup> in the diol partner. It is interesting that a seemingly minor skeletal variation in



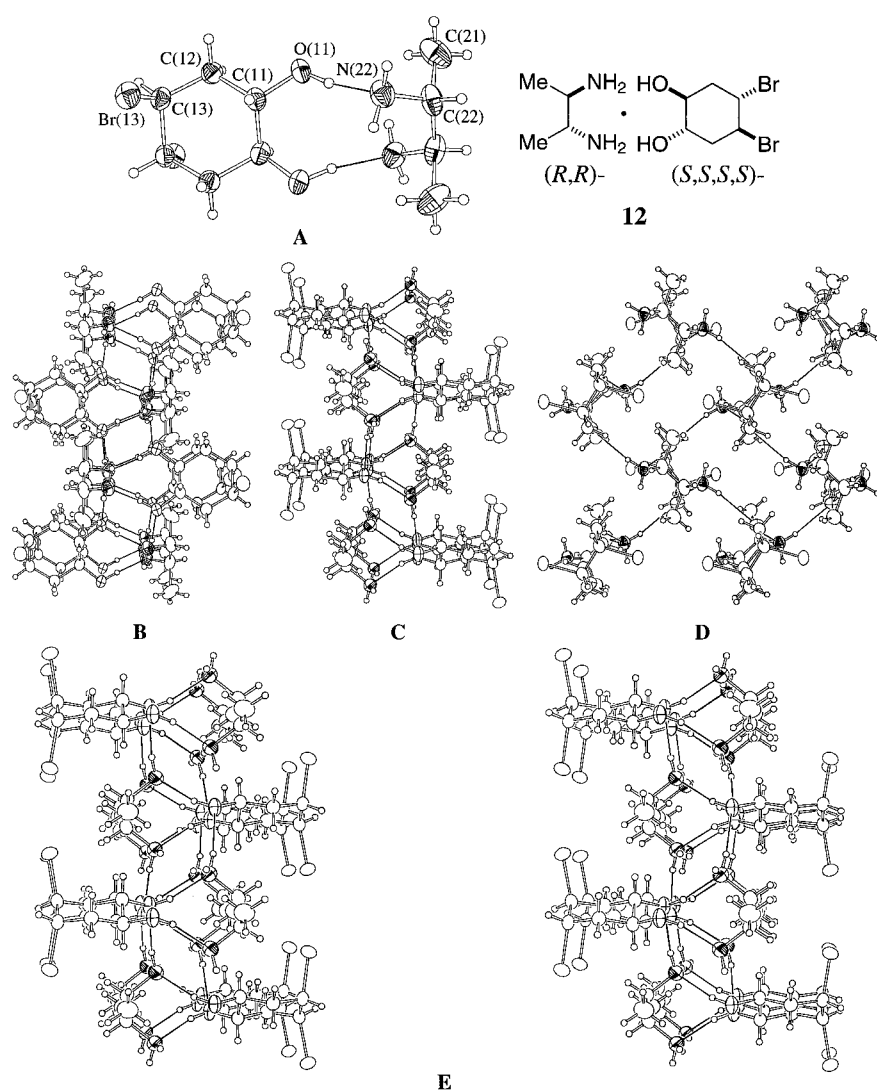


Figure 7. A) ORTEP view of the molecular adduct **12** (H-bonds are represented by thin lines); B) H-bonding network of adduct **12** (top view down the *a* axis); C) side view of the H-bonding network (H-bonds are represented by thin lines) showing the coordination of oxygen and nitrogen atoms and the spatial proximity of the inter-residue bromine atoms; D) single strand for H-bonded units extracted from the interlinked bidirectional hydrogen-bonding network in **12** along the *c* axis showing the tweezer-shaped motif. H-bonds are uniformly established between  $\text{NH}_2$  donors and OH acceptors of alternate diamine and diol molecules; E) stereoview of the H-bonding network (side view along the *b* axis).

the diol partner in **3**, **17**, and **15** can result in a drastically changed inner-core architecture. The three-dimensional structures of the supraminols could be the consequence of thermodynamically driven phenomena involving symmetry, steric, geometric, and electronic effects. Investigations of the binding affinities between vicinal diamines and diols by microcalorimetry have shown unexpected differences between diastereomeric complexes.<sup>[26]</sup> Preferences for  $\text{O} \rightarrow \text{N}$  hydrogen bonds rather than  $\text{N} \rightarrow \text{O}$  hydrogen bonds were predicted and rationalized based on enthalpic considerations. Furthermore, the thermodynamic parameters for *R,R* and *R,S* pairs of diamines and diols were found to be different, with the heterochiral pair being twice as favored on the basis of enthalpic considerations, but less favored entropically. From the data so far available, it is not possible to predict unequivocally if a particular diamine–diol motif will undergo

self-assembly to a helical or different spatial arrangement. Equally unpredictable is the prospect of obtaining solid adducts suitable for X-ray analysis. However, even with the relatively limited examples shown in this study, it is possible to make some logical predictions regarding the architecture of supraminols from a knowledge of the structures of the interacting components. For example, it is clear that the stereochemical information encoded in the (*R,R*)-diamine **1** leads to preferential recognition of (*R,R*)-diols rather than (*S,S*)-diols, and ultimately to self-assembly. It is fortuitous that the homochiral adducts **3** and **5** were obtained as crystalline solids, while the corresponding heterochiral adducts **19** and **20** were obtained as oils. On the other hand, the adducts of (*R,R*)-2,3-diaminobutane (**6**) with enantiomeric diols **4** and **11** were nicely crystalline (Scheme 1).

Adduct **10** is characterized by the presence of a vast hydrogen-bonding network, through which a three-dimensional structure assembles along the crystallographic *a* axis with a right-handed helical hydrogen-bonded ribbon-shaped core motif (Figure 6). Adduct **12**, formed from the enantiomeric diol **11**, is characterized by a highly interlinked bidirectional hydrogen-bonding network

that comprises an incompletely hydrogen-bonded core motif (Figure 7). This contrasts with the diastereomeric adducts **15** and **15a**, both of which are helical but with opposite senses of chirality, and with a pleated-sheet-like hydrogen-bonded core (Table 2).<sup>[16]</sup> Why then should there be such a diversity in three-dimensional architecture and core structure of adducts resulting from the same diamine and a diol or its enantiomer? (e.g. adducts **5** and **20**, **10** and **12**, **15** and **15a**, Schemes 1 and 3, Table 2, Figure 10). Although torsional angles and geometric parameters between acyclic and cyclic diamines (e.g. **1** and **6**) and diol partners could be in part responsible for the different core structures, the differences are not so distinct as to permit definitive predictions (Table 2). Rather, the better matched pairs may be thermodynamically much more stable, especially when the adduct crystallizes out preferentially. Curiously, when **1** and racemic *trans*-cyclohexane 1,2-diol are heated in

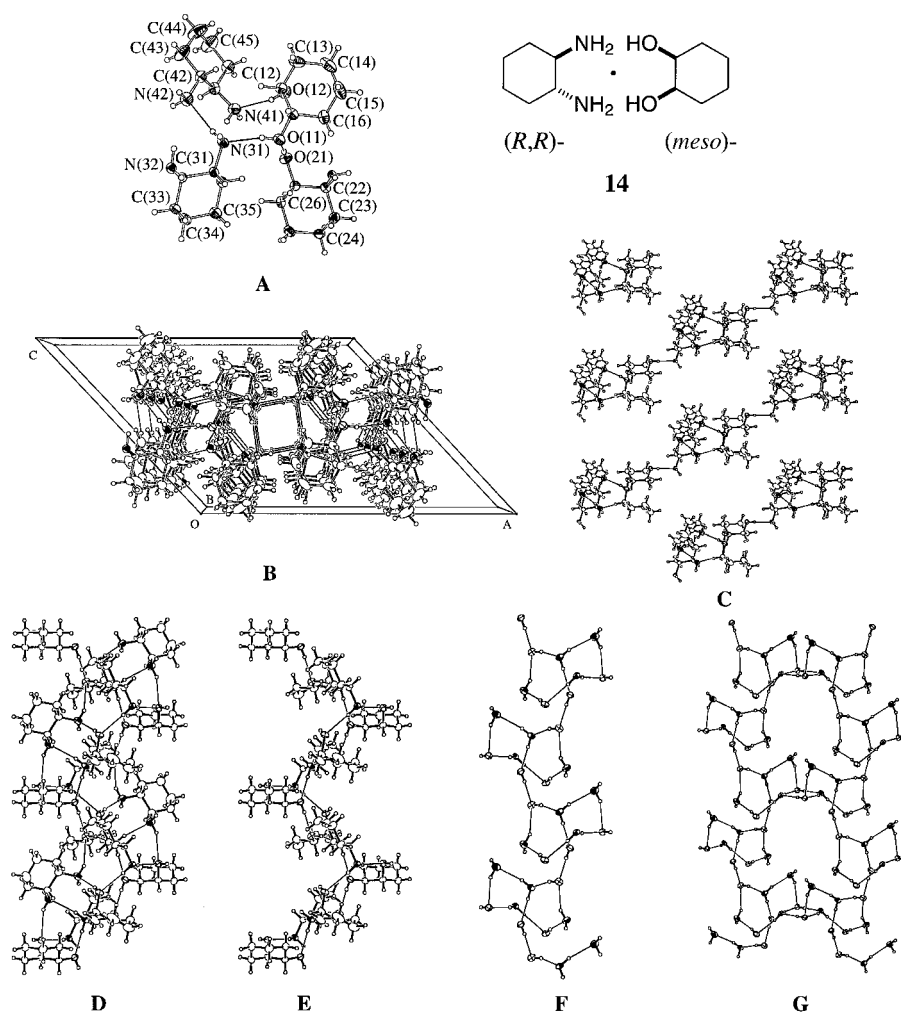
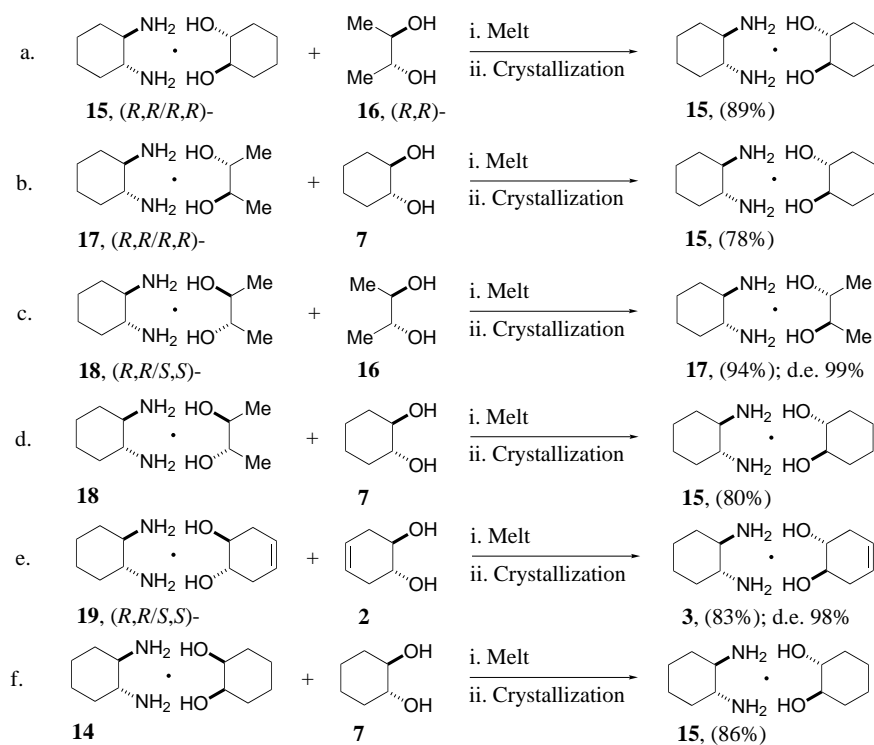


Figure 8. A) ORTEP view of the dimeric molecular adduct **14** (H-bonds are represented by thin lines); B) H-bonding network of adduct **14** (top view down the *b* axis); C) H-bonding network linking columns of dimeric units (H-bonds are represented by thin lines); D) side view of the H-bonding network within one dimeric column; E) single strand for H-bonded units extracted from the two dimensional network in D; F) simplified representation of the view in D showing the incomplete right-handed ribbon motif of the H-bonded core of the assembly; G) right-handed incomplete ribbon motifs of two columns of dimeric units with interlinked square planar H-bonds.

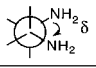
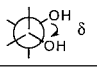
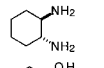
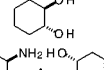
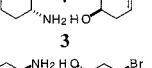
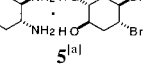
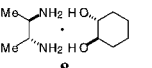
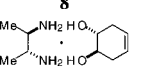
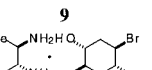
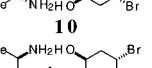
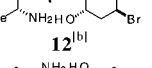
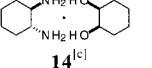
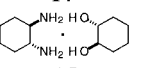
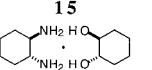


Scheme 2. Competition experiments to evaluate the relative stability of supraminols.

refluxing benzene, the homo-chiral adduct **15** crystallizes out preferentially, while **15a** remains in the mother liquor (Table 2).<sup>[16, 25a]</sup> Competition experiments also show that **15** appears to consist of the preferred matched chiron combination given the choice of diol partners.

One would have intuitively presumed a preference for diamine **1** to incorporate a fully hydrogen-bonded core as found in adduct **17** (m.p. 63–65 °C) given the choice between the acyclic and cyclic diols **16** and **7**. Competition experiments reveal that preference goes to **7** to give the adduct **15** (m.p. 78–79 °C) in which the core is only partially hydrogen-bonded as a pleated-sheet motif (Scheme 2).

Table 2.  $\delta$  angle values and inter-residue distances for repeating helical units (pitch).

Adduct	mp [°C]			Core motif	Pitch [Å]	Helix type
	41–43	–59.2	–	–	–	–
	107–109	–	–60.8	–	–	–
	58–60	–55.5	–57.3	ribbon	20.18	left-handed
	64–66	–53.9	–63.0 –61.0	ribbon	19.52	left-handed
	42–44	–48.9	–58.5	ribbon	20.34	left-handed
	64–66	–49.0	–53.7	ribbon	20.21	left-handed
	78–80	–54.4	–69.7	ribbon	19.30	left-handed
	64–66	+62.5	+66.0	tweezer	7.92	–
	44–46	–56.4 –60.3	–57.4 –56.0	incomplete ribbon	11.52	–
	78–79	–57.4	–63.5	pleated sheet	15.72	left-handed
	63–65	–57.8	+60.1	pleated sheet	15.05	right-handed
	63–65	–56.1	–54.6	ribbon	20.29	left-handed

[a] Ordered diamine. [b]  $C_2$  symmetric. [c] Double asymmetric unit (two diols and two diamines).

Table 3. Difference in  $^1\text{H}$  NMR chemical shift  $\delta$  for  $\text{CHOH}$ ,  $\text{CHNH}_2$ ,  $\text{ROH}$ , and  $\text{RNH}_2$  [ppm].

Entry	Adduct	$\Delta\Delta^{[a]}$ $\text{CHOH}$	$\Delta\Delta^{[b]}$ $\text{CHOH}$	$\Delta\Delta^{[a]}$ $\text{CHNH}_2$	$\Delta\Delta^{[b]}$ $\text{CHNH}_2$	$\Delta\Delta^{[a]}$ $\text{ROH}$	$\Delta\Delta^{[b]}$ $\text{RNH}_2$	$\Delta\Delta^{[a]}$
1	<b>3</b>	+0.30	+0.18	+0.08	+0.07	–2.20	+1.04	
2	<b>5</b>	+0.38	+0.18	+0.08	+0.08	–0.80	+0.99	
3	<b>8</b>	+0.12	+0.10	+0.08	+0.15	–0.39	–0.27	
4	<b>9</b>	+0.18	+0.11	+0.20	+0.20	–2.38	–0.23	
5	<b>10</b>	+0.21	+0.10	+0.20	+0.23	–1.18	–0.48	
6	<b>12</b>	+0.24	+0.12	+0.28	+0.25	–0.40	–0.30	
7	<b>14</b>	+0.18	+0.10	+0.10	+0.07	–0.57	+0.52	
8	<b>15</b>	+0.10	+0.06	+0.08	+0.07	–0.30	+0.54	
9	<b>17</b>	+0.15	+0.08	+0.08	+0.08	–0.32	+0.64	
10	<b>19</b>	+0.31	+0.14	+0.24	+0.06	–1.45	+1.79	
11	<b>20</b>	+0.39	+0.14	+0.04	+0.07	–0.57	+1.22	
12	<b>21</b>	+0.18	+0.08	+0.15	+0.18	–0.30	+1.94	
13	<b>22</b>	+0.14	+0.07	+0.08	+0.07	–0.80	+0.86	
14	<b>24</b> <sup>[c]</sup>	+0.36	–0.07	+0.09	–0.01	+0.98	+1.22	
15	<b>25</b> <sup>[c]</sup>	+0.11	+0.02	–0.02	–0.03	– <sup>[d]</sup>	– <sup>[d]</sup>	
16	<b>26</b> <sup>[c]</sup>	+0.22	–0.03	–0.04	0.00	– <sup>[d]</sup>	– <sup>[d]</sup>	
17	<b>27</b> <sup>[c]</sup>	– <sup>[e]</sup>	–0.14 <sup>[f]</sup>	– <sup>[e]</sup>	–0.40 <sup>[f]</sup>	–1.75 <sup>[b]</sup>	+1.75 <sup>[b]</sup>	

[a] Spectra were recorded in 0.1M [ $D_6$ ]benzene solution at 25 °C. [b] Spectra were recorded in 0.1M  $\text{CDCl}_3$  solution at 25 °C. [c]  $^1\text{H}$  NMR spectra recorded with equimolar amount of alcohol and amine. [d] Signal overlap. [e] Adduct insoluble in benzene. [f]  $\beta$ -Hydrogen.

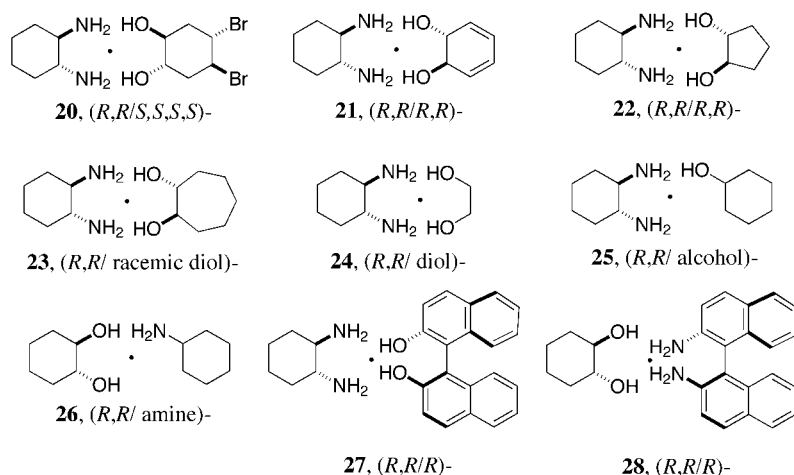
From a comparison of the values of the pitch in Å of the helical strands in homo- and heterochiral adducts (Table 2), it appears that a more compact helical structure is associated with adduct **15a** (pitch 15.05 Å). This would tempt one to assume that it would also be the more stable supra-molecular chiron with a shorter averaged hydrogen-bonded network throughout the assembly. Direct competition between **7** and its enantiomer in combination with the diamine **1** leads to the preferential crystallization of the higher melting, slightly more elongated helical adduct **15**. The preference for crystallization of the homochiral  $R,R$  complex **15** over the heterochiral  $R,S$  pair **15a** is intriguing in view of the prediction from microcalorimetry that the heterochiral complex is energetically more favored.<sup>[26]</sup> It appears that entropy rather than enthalpy plays a more important role in the pairing of homochiral diamines and diols compared to the heterochiral counterparts. Thus, the slightly more elongated architecture of complex **15** (pitch 15.72 Å) may be entropically more favored than the more compact **15a** (pitch 15.05 Å) in the context of a supramolecular structure. Clearly, it is not possible to make definitive predictions regarding the stability of a given adduct based solely on its crystallization properties and the limited physical data we have gathered so far.

The geometry of the diol (*cis* vs. *trans* stereochemistry) shows an important directional effect in the organization of supraminols. In fact, in the adduct formed from the achiral diol **13** and **1**, a markedly different hydrogen-bonded neutral network is observed. Two diamine and two diol molecules are necessary to define the elemental crystallographic unit cell which extends into a layered structure with incompletely hydrogen-bonded ribbon-shaped cores (Figure 8). The presence of two supplementary diol and diamine molecules in the elemental unit cell is probably necessary to compensate for the lack of  $C_2$  symmetry in the recognition process, as opposed to adduct **15**, for example.

The inclusion of a molecule of benzene in the adduct **9** (Figures 2, 5) represents an interesting example of host-guest chemistry in three-dimensional assemblies in which an aromatic hydrocarbon is involved without stacking interactions.<sup>[22]</sup> Of interest is the alignment of the benzene rings in a plane parallel to the axis of the helical columns that comprise the crystallographic unit, and the exclusion of toluene when it was present during the crystallization process.

## Conclusion

We have shown that  $C_2$ -symmetrical vicinal diamines and *functionalized* diols can form stable supramolecular adducts which we have called *supraminols*. In general, the



Scheme 3. The structures of diamine–diol and diamine–alcohol adducts prepared from equimolar quantities of the reagents.

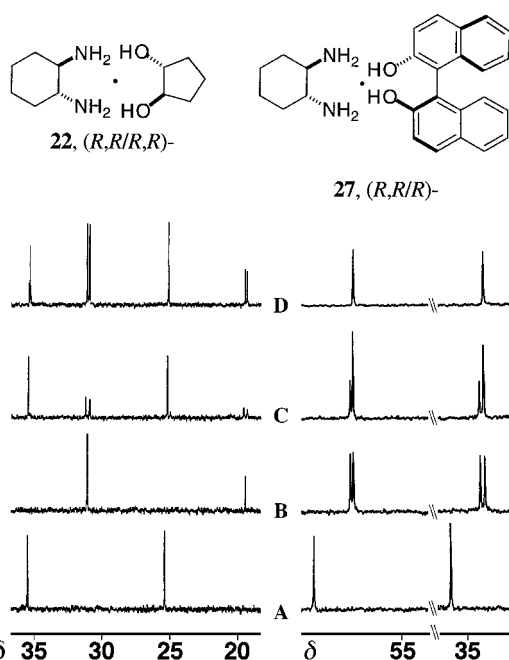


Figure 9. Partial  $^{13}\text{C}$  NMR spectra (0.2 M  $\text{CDCl}_3$ ) for **22** and **27**. For **22**: A) (*R,R*)-1,2-diaminocyclohexane; B) *trans*-( $\pm$ )-1,2-cyclopentenediol; C) 1:1 adduct between (*R,R*)-1,2-diaminocyclohexane and *trans*-( $\pm$ )-1,2-cyclopentenediol showing molecular recognition and chiral discrimination of the diastereomeric supraminols; D) 0.5:1 adduct between (*R,R*)-1,2-diaminocyclohexane and *trans*-( $\pm$ )-1,2-cyclopentenediol showing selective molecular recognition and chiral discrimination of the supraminol **22**. For **27**: A) (*R,R*)-1,2-diaminocyclohexane; B) 1:1 adduct between (*R*)-1,1'-bi-2-naphthol and *trans*-( $\pm$ )-1,2-diaminocyclohexane showing molecular recognition and chiral discrimination of the diastereomeric supraminols; C) 1:1 adduct between (*R*)-1,1'-bi-2-naphthol and (*R,R*)-1,2-diaminocyclohexane (*ee* 35%) showing molecular recognition and chiral discrimination of the diastereomeric supraminols; D) 1:1 adduct between (*R*)-1,1'-bi-2-naphthol and (*R,R*)-1,2-diaminocyclohexane (**27**).

stereochemical information encoded in these acyclic and cyclic vicinal diamines is reflected in their preference for stereochemically matched diols to give homoadducts. This aspect of functional and molecular recognition through hydrogen bonding between amino and hydroxyl groups was

further confirmed by competition experiments in which homoadducts were formed from heteroadducts by exchange with the better matching diol partner. As a result, enantiomeric enrichment of racemic mixtures of diols or diamines is possible. While it is clear that a number of vicinal  $C_2$ -symmetrical diamines and diols will self-assemble, it is not possible at present to predict the three-dimensional architecture of the assembly with a high degree of confidence. Within the family of *trans*-2,3-diaminobutanes and *trans*-1,2-diaminocyclohexanes, however, prospects of

forming helical assemblies with matching homochiral cyclic and acyclic vicinal diols are excellent. The left- or right-handed helicity of such three-dimensional assemblies is also predictable within a given series. In general, a (*R,R*)-diamine and the corresponding homochiral (*R,R*)-diol will give rise to a left-handed helical shape.

It is more difficult to predict the three-dimensional architecture of the hydrogen-bonded core motifs of these helical supraminols. There appears to be a preference for a ribbon-shaped hydrogen-bonded structure in the case of functionalized diols (Figure 10). In the absence of steric constraints, the amine and alcohol groups are engaged in hydrogen bonding; otherwise partial association through hydrogen bonds is observed while the integrity of the ribbonlike architecture is maintained.

It is of interest to point out that while the outer architecture of the (*R,R*)-supraminols **3**, **5**, **8**, **9**, and **10** portrays left-handed helicity that of the inner core ribbon-shaped motif is of the opposite sense. Through the power of hydrogen bonding we have thus created supramolecular assemblies that are endowed with and encoded for two types of distinct helical motifs within one structure.

In the case of adducts **15** and **15a**<sup>[16]</sup> (Table 2), the outer architectures show left- and right-handed helicity, respectively, simply by changing the sense of chirality of one of the partners. The inner core consists of a pleated-sheet hydrogen-bonded structure. It is of interest to point out that nature has selected among its many three-dimensional arrays of molecular shapes the helix and the  $\beta$ -sheet as part of its mechanisms for recognition and catalysis in life processes.<sup>[27]</sup>

Finally, it may be compelling to address the origin of the process by which supraminols self-assemble. To this end, we suggest the following possibilities. Firstly, an enantiomer-differentiating recognition between a diamine and a matching diol to give a supramolecular chiron (e.g. Figure 1A), followed by interlinking through a network of hydrogen bonds to produce the supramolecular assembly in its thermodynamically most stable architecture. Alternatively, matching diol molecules could insert in the layered two-dimensional lattice of the diamine **1**, followed by association through hydrogen bonding

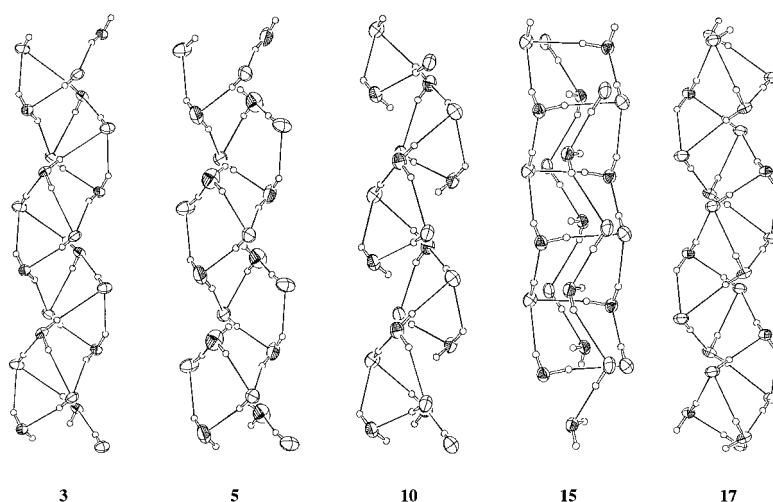


Figure 10. Comparison between core H-bonded structures for supraminols **3**, **5**, **10**, **15**, and **17** showing right-handed core ribbon motif and a pleated-sheet staircaselike motif (**15**).

and building the assembly. The competition experiments in solution showing the preference for a particular diol partner over an existing one in a preformed supraminol further demonstrate the importance of thermodynamic and other considerations in the assembly of the supraminols. Under the nonpolar conditions of the interaction, a strong driving force is to orient all the polar groups in a mutually complementary manner resulting in maximum coordination through hydrogen bonding. There seems to be no particular preference for O→N or N→O hydrogen bonds, contrary to predictions based on microcalorimetry.<sup>[26]</sup>

Clearly, more examples with additional functional and geometric variations are needed to lay a deeper foundation for our understanding of the factors governing three-dimensional molecular architectures in the supraminol family of superstructures. Studies towards these goals, in conjunction with exploiting possible applications of supraminols in catalysis, in solid-state chemistry and related areas of interest are in progress.

## Experimental Section

**General methods:** All the starting materials used were commercial products whose physical constants were in agreement with reported values. Compound **1** was obtained by a resolution process described in refs. [16, 18]. Compound **6** was synthesized with the procedure reported in ref. [21]. Compounds **2**, **4**, and **11** were synthesized using the procedure reported in ref. [19]. Melting-point determinations are uncorrected. NMR spectra were recorded at 300 and 400 MHz for <sup>1</sup>H and at 75 and 100 MHz for <sup>13</sup>C. For details of X-ray structure determination<sup>[20]</sup> and additional data, please contact the author.

**General procedure for preparing adducts:** Equimolar quantities of diamines **1** and **6** and appropriate diols were suspended in dry benzene, and the suspension was heated to boiling point on a hot plate. The homogeneous solution was allowed to cool to room temperature. The crystalline adducts that formed were filtered and recrystallized from benzene. In the case of oils, they were dried under high vacuum and directly characterized.

**Adduct between (R,R)-1,2-diaminocyclohexane and (R,R)-cyclohexan-1,2-diol (3):**<sup>[19]</sup> Colorless needles, m.p. 58–60 °C,  $[\alpha]_D^{25} = -77.02$  ( $c = 1$ , CDCl<sub>3</sub>), <sup>1</sup>H NMR (300 MHz, CDCl<sub>3</sub>, 0.1M):  $\delta = 1.05$  (m, 2H,

CH<sub>2</sub>CH<sub>2</sub>CHNH), 1.28 (m, 2H, CH<sub>2</sub>CH<sub>2</sub>CHNH), 1.64 (m, 2H, CH<sub>2</sub>CHNH), 1.80 (m, 2H, CH<sub>2</sub>CHNH), 2.01 (m, 2H, CH<sub>2</sub>CHOH), 2.22 (m, 2H, CHNH), 2.43 (m, 6H, OH+NH<sub>2</sub>), 3.51 (m, 2H, CHO), 5.50 (m, 2H, CH=CH); <sup>13</sup>C NMR (300 MHz, CDCl<sub>3</sub>, 0.1M):  $\delta = 25.05$  (CH<sub>2</sub>CH<sub>2</sub>CHNH), 33.0 (CH<sub>2</sub>CHOH), 35.50 (CH<sub>2</sub>CHNH), 57.0 (CHNH), 71.05 (CHO), 124.95 (CH=CH).

**Adduct between (R,R)-1,2-diaminocyclohexane and (1R,2R,4R,5R)-4,5-dibromocyclohexan-1,2-diol (5):**<sup>[19]</sup>

Colorless needles, m.p. 64–66 °C,  $[\alpha]_D = -44.63$  ( $c = 0.64$ , CDCl<sub>3</sub>); <sup>1</sup>H NMR (300 MHz, CDCl<sub>3</sub>, 0.1M):  $\delta = 1.10$  (m, 2H, CH<sub>2</sub>CH<sub>2</sub>CHNH), 1.30 (m, 2H, CH<sub>2</sub>CH<sub>2</sub>CHNH), 1.70 (m, 2H, CH<sub>2</sub>CHNH), 1.85 (m, 2H, CH<sub>2</sub>CHNH), 2.28 (m, 2H, CHNH), 2.40 (m, 8H, CH<sub>2</sub>CHOH+OH+NH<sub>2</sub>), 2.50 (m, 2H, CH<sub>2</sub>CHOH), 3.95 (m, 2H, CHBr), 4.51 (m, 2H, CHO); <sup>13</sup>C NMR (300 MHz, CDCl<sub>3</sub>, 0.1M):  $\delta = 25.10$  (CH<sub>2</sub>CH<sub>2</sub>CHNH), 35.30 (CH<sub>2</sub>CHOH), 35.90 (CH<sub>2</sub>CHNH), 51.10 (CHBr), 57.10 (CHNH), 70.30 (CHO).

**Adduct between (R,R)-2,3-diaminobutane<sup>[21]</sup> and (R,R)-cyclohexane-1,2-diol (8):** Colorless needles, m.p. 42–44 °C,  $[\alpha]_D = -53.33$  ( $c = 0.43$ , CDCl<sub>3</sub>); <sup>1</sup>H NMR (400 MHz, CDCl<sub>3</sub>, 0.1M):  $\delta = 1.08$  (d,  $J = 7.0$  Hz, 3H, CH<sub>3</sub>), 1.38 (m, 4H, CH<sub>2</sub>CH<sub>2</sub>CHOH), 1.71 (m, 2H, CH<sub>2</sub>CHOH), 1.95 (m, 2H, CH<sub>2</sub>CHOH), 2.20 (brs, 6H, OH+NH<sub>2</sub>), 2.63 (m, 2H, CHNH), 3.30 (m, 2H, CHO); <sup>13</sup>C NMR (300 MHz, CDCl<sub>3</sub>, 0.1M):  $\delta = 20.70$  (CH<sub>3</sub>), 24.26 (CH<sub>2</sub>), 32.79 (CH<sub>2</sub>), 52.86 (CH), 75.54 (CH).

**Adduct between (R,R)-2,3-diaminobutane<sup>[21]</sup> and (R,R)-4-cyclohexen-1,2-diol (9):**<sup>[20]</sup> Colorless needles, m.p. 64–66 °C,  $[\alpha]_D = -70.56$  ( $c = 0.85$ , CDCl<sub>3</sub>); <sup>1</sup>H NMR (400 MHz, CDCl<sub>3</sub>, 0.1M):  $\delta = 1.0$  (d,  $J = 7.0$  Hz, 3H, CH<sub>3</sub>), 2.05 (m, 2H, CH<sub>2</sub>CHOH), 2.22 (brs, 6H, OH+NH<sub>2</sub>), 2.47 (m, 2H, CH<sub>2</sub>CHOH), 2.68 (m, 2H, CHNH), 3.64 (m, 2H, CHNH), 5.53 (m, 2H, CH=CH); <sup>13</sup>C NMR (400 MHz, CDCl<sub>3</sub>, 0.1M):  $\delta = 20.77$  (CH<sub>3</sub>), 33.35 (CH<sub>2</sub>), 52.88 (CH), 71.81 (CH), 124.49 (C=CH).

**Adduct between (R,R)-2,3-diaminobutane<sup>[21]</sup> and (1R,2R,3R,5R)-4,5-dibromocyclohexan-1,2-diol (10):**<sup>[20]</sup> Colorless needles, m.p. 78–80 °C,  $[\alpha]_D = -34.75$  ( $c = 0.61$ , CDCl<sub>3</sub>); <sup>1</sup>H NMR (400 MHz, CDCl<sub>3</sub>, 0.1M):  $\delta = 1.05$  (d,  $J = 7.0$  Hz, 6H, CH<sub>3</sub>), 1.95 (brs, 6H, OH+NH<sub>2</sub>), 2.30 (m, 4H, CH<sub>2</sub>CHOH), 2.53 (m, 2H, CH<sub>2</sub>CHOH), 2.65 (m, 2H, CHNH), 3.98 (m, 2H, CHBr), 4.63 (m, 2H, CHO); <sup>13</sup>C NMR (300 MHz, CDCl<sub>3</sub>, 0.1M):  $\delta = 20.86$  (NCH<sub>3</sub>), 35.43 (CH<sub>2</sub>CHOH), 51.31 (CHBr), 52.82 (CHNH), 70.71 (CHO).

**Adduct between (R,R)-2,3-diaminobutane<sup>[21]</sup> and (1R,2R,3R,5R)-4,5-dibromocyclohexan-1,2-diol (12):**<sup>[19]</sup> Colorless needles, m.p. 64–66 °C,  $[\alpha]_D = -13.33$  ( $c = 1.50$ , CDCl<sub>3</sub>); <sup>1</sup>H NMR (400 MHz, CDCl<sub>3</sub>, 0.1M):  $\delta = 1.05$  (d,  $J = 7.0$  Hz, 6H, CH<sub>3</sub>), 2.30 (m, 4H, CH<sub>2</sub>CHOH), 2.58 (m, 2H, CHNH), 2.74 (brs, 6H, OH+NH<sub>2</sub>), 3.92 (m, 2H, CHBr), 4.59 (m, 2H, CHO); <sup>13</sup>C NMR (300 MHz, CDCl<sub>3</sub>, 0.1M):  $\delta = 21.10$  (NCH<sub>3</sub>), 39.99 (CH<sub>2</sub>CHOH), 55.87 (CHBr), 57.33 (CHNH), 75.16 (CHO).

**Adduct between (R,R)-1,2-diaminocyclohexane and cis-cyclohexan-1,2-diol (14):** Colorless needles, m.p. 44–46 °C,  $[\alpha]_D = -18.05$  ( $c = 0.72$ , CDCl<sub>3</sub>); <sup>1</sup>H NMR (300 MHz, CDCl<sub>3</sub>, 0.1M):  $\delta = 1.20$  (m, 8H, CH<sub>2</sub>CH<sub>2</sub>CHNH and CH<sub>2</sub>CH<sub>2</sub>CHOH), 1.75 (m, 8H, CH<sub>2</sub>CHNH and CH<sub>2</sub>CHOH), 2.03 (brs, 6H, OH+NH<sub>2</sub>), 2.26 (m, 2H, CHNH), 3.72 (m, 2H, CHO); <sup>13</sup>C NMR (300 MHz, CDCl<sub>3</sub>, 0.1M):  $\delta = 21.10$  (CH<sub>2</sub>CH<sub>2</sub>CHOH), 25.24 (CH<sub>2</sub>CH<sub>2</sub>CHNH), 29.28 (CH<sub>2</sub>CHOH), 35.42 (CH<sub>2</sub>CHNH), 57.37 (CHNH), 71.05 (CHO), 124.95 (CH=CH).

**Adduct between (R,R)-1,2-diaminocyclohexane and (S,S)-cyclohexen-1,2-diol (19):**<sup>[19]</sup> Oil; <sup>1</sup>H NMR (300 MHz, CDCl<sub>3</sub>, 0.1M):  $\delta = 1.05$  (m, 2H, CH<sub>2</sub>CH<sub>2</sub>CHNH), 1.28 (m, 2H, CH<sub>2</sub>CH<sub>2</sub>CHNH), 1.62 (m, 2H, CH<sub>2</sub>CHNH), 1.81 (m, 2H, CH<sub>2</sub>CHNH), 2.02 (m, 2H, CH<sub>2</sub>CHOH), 2.22 (m, 2H, CHNH), 3.05 (m, 6H, OH+NH<sub>2</sub>), 3.49 (m, 2H, CHO), 5.50 (m, 2H, CH=CH); <sup>13</sup>C NMR (300 MHz, CDCl<sub>3</sub>, 0.1M):  $\delta = 25.05$  (CH<sub>2</sub>CH<sub>2</sub>CHNH), 33.10

( $CH_2CHOH$ ), 35.50 ( $CH_2CHNH$ ), 57.2 (CHNH), 71.06 (CHOH), 124.95 (CH=CH).

**Adduct between (R,R)-1,2-diaminocyclohexane and (1S,2S,4S,5S)-4,5-dibromocyclohexane-1,2-diol (20):**<sup>[19]</sup> Oil, <sup>1</sup>H NMR (300 MHz, CDCl<sub>3</sub>, 0.1M): δ = 1.10 (m, 2H,  $CH_2CH_2CHNH$ ), 1.30 (m, 2H,  $CH_2CH_2CHNH$ ), 1.70 (m, 2H,  $CH_2CHNH$ ), 1.92 (m, 2H,  $CH_2CHNH$ ), 2.25 (m, 2H, CHNH), 2.42 (m, 8H,  $CH_2CHOH+OH+NH_2$ ), 2.58 (m, 2H,  $CH_2CHOH$ ), 3.96 (m, 2H, CHBr), 4.55 (m, 2H, CHOH); <sup>13</sup>C NMR (300 MHz, CDCl<sub>3</sub>, 0.1M): δ = 25.0 ( $CH_2CH_2CHNH$ ), 34.48 ( $CH_2CHOH$ ), 35.90 ( $CH_2CHNH$ ), 51.15 (CHBr), 57.11 (CHNH), 70.32 (CHOH).

**Adduct between (R,R)-1,2-diaminocyclohexane and (R,R)-3,5-cyclohexadiene-1,2-diol (21):**<sup>[19]</sup> Oil, <sup>1</sup>H NMR (300 MHz, CDCl<sub>3</sub>, 0.1M): δ = 1.12 (m, 2H,  $CH_2CH_2CHNH$ ), 1.21 (m, 2H,  $CH_2CH_2CHNH$ ), 1.63 (m, 2H,  $CH_2CHNH$ ), 1.81 (m, 2H,  $CH_2CHNH$ ), 2.33 (m, 2H, CHNH), 3.30 (brs, 6H, OH+NH<sub>2</sub>), 4.42 (s, 2H, CH), 5.80 (s, 2H, CH); <sup>13</sup>C NMR (300 MHz, CDCl<sub>3</sub>, 0.1M): δ = 25.5 ( $CH_2CH_2CHNH$ ), 35.32 ( $CH_2CHNH$ ), 56.82 (CHNH), 74.51 (CHOH), 123.78 (CH), 131.4 (CH).

**Adduct between (R,R)-1,2-diaminocyclohexane and (R,R)-cyclopentane-1,2-diol (22):**<sup>[20]</sup> Oil, <sup>1</sup>H NMR (300 MHz, CDCl<sub>3</sub>, 0.1M): δ = 1.10 (m, 2H,  $CH_2CH_2CHNH$ ), 1.20 (m, 2H,  $CH_2CH_2CHNH$ ), 1.40 (m, 2H,  $CH_2CH_2CHOH$ ), 1.65 (m, 4H,  $CH_2CHNH$  and  $CH_2CHOH$ ), 1.70 (m, 2H,  $CH_2CHOH$ ), 1.80 (m, 2H,  $CH_2CHNH$ ), 2.20 (brs, 8H,  $CH_2CHOH$ ), 3.90 (m, 2H, CHOH), 5.50 (m, 2H, CH=CH); <sup>13</sup>C NMR (300 MHz, CDCl<sub>3</sub>, 0.1M): δ = 19.7 ( $CH_2CH_2CHOH$ ), 25.21 ( $CH_2CH_2CHNH$ ), 31.19 ( $CH_2CHOH$ ), 35.39 ( $CH_2CHNH$ ), 57.27 (CHNH), 78.79 (CHOH).

**General procedure for the competition experiments:** Equimolar quantities of the crystalline adduct and the appropriate diol were suspended in dry benzene, and the suspension was heated to the boiling point on a hot plate. The homogeneous solution was allowed to cool to room temperature, whereupon crystalline adducts were formed. These were filtered, recrystallized from benzene, and fully characterized by optical rotation and spectroscopic analyses.

## Acknowledgements

We thank NSERC for generous financial assistance. R.M. thanks the University of Rome La Sapienza for a fellowship.

- [1] For comprehensive treatises, see: J.-M. Lehn, *Supramolecular Chemistry*, VCH, Weinheim, Germany, **1995**; *Comprehensive Supramolecular Chemistry, Vol. 11* (Eds.: J. L. Atwood, J. E. D. Davies, D. D. MacNicol, F. Vögtle), Pergamon, Oxford, **1996**.
- [2] J.-M. Lehn, *Angew. Chem.* **1990**, *102*, 1347; *Angew. Chem. Int. Ed. Engl.* **1990**, *29*, 1304; J.-M. Lehn, *Angew. Chem.* **1988**, *100*, 91; *Angew. Chem. Int. Ed. Engl.* **1988**, *27*, 89.
- [3] A. Gavezzotti, G. Filippini, *Chem. Commun.* **1998**, 287; M. Mascal, *Contemp. Org. Synth.* **1994**, *1*, 31; C. B. Aakeröy, K. R. Seddon, *Chem. Soc. Rev.* **1993**, *22*, 397; F. J. DiSalvo, *Science* **1990**, *247*, 649.
- [4] G. R. Desiraju, *Angew. Chem.* **1995**, *107*, 2541; *Angew. Chem. Int. Ed. Engl.* **1995**, *34*, 2311; S. Subramanian, M. J. Zaworotko, *Coord. Chem. Rev.* **1994**, *137*, 957; G. R. Desiraju, *Crystal Engineering, The Design of Organic Solids*, Elsevier, New York, **1989**.
- [5] See for example: J. C. MacDonald, G. M. Whitesides, *Chem. Rev.* **1994**, *94*, 2383; V. Videnova-Adrabsinska, *J. Mol. Struct.* **1996**, *374*, 199; A. E. Rowan, R. J. M. Nolte, *Angew. Chem.* **1998**, *110*, 71; *Angew. Chem. Int. Ed. Engl.* **1998**, *37*, 63.
- [6] For pertinent references on predictions of crystal structures, see: G. R. Desiraju, *Science* **1997**, *278*, 404; A. Gavezzotti, *Acc. Chem. Res.* **1994**, *27*, 309; J. Perlstein, *J. Am. Chem. Soc.* **1994**, *116*, 455; J. Perlstein, *J. Am. Chem. Soc.* **1992**, *114*, 1955; A. Gavezzotti, *J. Am. Chem. Soc.* **1991**, *113*, 4622; M. C. Etter, *Acc. Chem. Res.* **1990**, *23*, 120; J. Maddox, *Nature* **1988**, *335*, 201; L. Leiserowitz, A. T. Hagler, *Proc. R. Soc. London A* **1988**, *388*, 133; D. Y. Curtin, I. C. Paul, *Chem. Rev.* **1981**, *81*, 525.
- [7] For a scholarly treatise, see: E. J. Corey, X.-M. Cheng, *The Logic of Chemical Synthesis*, Wiley, New York, **1989**; for other perspectives see: S. Hanessian, *Total Synthesis of Natural Products, The Chiron Approach*, Pergamon, New York, **1983**; S. Hanessian, *Aldrichimica Acta* **1989**, *22*, 3.
- [8] See for example: F. Frankel, G. M. Whitesides, *On the Surface of Things*, Chronicle, San Francisco, CA, **1997**; I. Hargittai, M. Hargittai, *Symmetry through the Eyes of a Chemist*, VCH, New York, **1986**.
- [9] See for example: M. D. Joesten, L. J. Schaad, *Hydrogen Bonding*, M. Dekker, New York, **1974**, p. 272; M. C. R. Symons, *Chem. Soc. Rev.* **1983**, *12*, 1; H. S. Aaron, *Top. Stereochem.* **1979**, *11*, 1; M. C. Etter, *J. Phys. Chem.* **1991**, *95*, 4601; J. Bernstein, R. E. Davis, L. Shrimani, N. L. Chang, *Angew. Chem.* **1995**, *107*, 1689; *Angew. Chem. Int. Ed. Engl.* **1995**, *34*, 1555.
- [10] See for example: G. A. Jeffrey, W. Saenger, *Hydrogen Bonding in Biological Structures*, Springer, Berlin, **1991**; L. Pauling, *The Nature of the Chemical Bond*, 3rd ed., Cornell University Press, Ithaca, NY, **1960**.
- [11] For selected recent references, see: N. Khazanovich, J. R. Granja, D. E. McRee, R. A. Milligan, M. R. Ghadiri, *J. Am. Chem. Soc.* **1994**, *116*, 6011; J. P. Mathias, E. E. Simanek, G. M. Whitesides, *J. Am. Chem. Soc.* **1994**, *116*, 4326; J. P. Mathias, E. E. Simanek, J. A. Zerkowski, C. T. Seto, G. M. Whitesides, *J. Am. Chem. Soc.* **1994**, *116*, 4316; J. Yang, J.-L. Marendaz, S. J. Geib, A. D. Hamilton, *Tetrahedron Lett.* **1994**, *35*, 3665; J. Yang, E. Fan, S. J. Geib, A. D. Hamilton, *J. Chem. Soc.* **1993**, *115*, 5314; J.-M. Lehn, M. Mascal, A. DeCian, J. Fisher, *J. Am. Chem. Soc. Perkin Trans. 2* **1992**, 461; M. Simard, D. Su, J. D. Wuest, *J. Am. Chem. Soc.* **1991**, *113*, 4696, and references therein; for crystallographic studies, see: R. Taylor, O. Kennard, *Acc. Chem. Res.* **1984**, *17*, 320.
- [12] See for example: M. J. Tubergen, R. L. Kuczkowski, *J. Am. Chem. Soc.* **1993**, *115*, 9263; U. Edlund, C. Holloway, G. C. Levy, *J. Am. Chem. Soc.* **1976**, *98*, 5069. See also ref. [10].
- [13] J. H. Lehlin, K. J. Franz, L. Gist, R. H. Moore, *Acta Crystallogr.* **1998**, *354*, 695; F. Toda, S. Hyoda, K. Okada, K. Hirotsu, *J. Chem. Soc. Chem. Commun.* **1995**, 1531; D. Mootz, D. Brodallo, M. Wiebke, *Acta Crystallogr. Sect. C* **1989**, *45*, 754; D. M. Lee, K. E. Burnfield, J. Blackwell, *Biopolymers* **1984**, *23*, 111; D. M. Lee, J. Blackwell, M. H. Litt, *Biopolymers* **1983**, *22*, 1383; see also: B. Henrissat, R. H. Marchessault, M. G. Taylor, H. Chanzy, *Polym. Commun.* **1987**, *28*, 113.
- [14] W. H. Pirkle, T.-C. Puchapsky, *Chem. Rev.* **1989**, *87*, 347; G. R. Weisman in *Asymmetric Synthesis, Vol. 1* (Ed.: J. D. Morrison), Academic Press, New York, **1983**, p. 153.
- [15] O. Ermer, A. Eling, *J. Chem. Soc. Perkin Trans. 2* **1994**, 925.
- [16] S. Hanessian, M. Simard, S. Roelens, *J. Am. Chem. Soc.* **1995**, *117*, 7630; S. Hanessian, A. Gomtsyan, M. Simard, S. Roelens, *J. Am. Chem. Soc.* **1994**, *116*, 4495.
- [17] See for example: M. M. Green, N. C. Peterson, T. Sato, A. Teramoto, R. Cook, S. Lifson, *Science* **1995**, *268*, 1860; Y. Chang, M. West, F. W. Fowler, J. W. Lauer, *J. Am. Chem. Soc.* **1993**, *115*, 5991.
- [18] For recent review, see: Y. L. Bennani, S. Hanessian, *Chem. Rev.* **1997**, *97*, 3161; K. Onuma, T. Ito, A. Nakamura, *Bull. Chem. Soc. Jpn.* **1980**, *53*, 2012; F. Galsbøl, P. Steenbøl, G. Søndergaard, S. B. Sørensen, *Acta Chem. Scand.* **1972**, *26*, 3605; R. G. Asperger, C. F. Liu, *Inorg. Chem.* **1965**, *4*, 1492; F. M. Jaeger, L. Z. Bijkerk, *Anorg. Allg. Chem.* **1937**, 233, 97.
- [19] H. Suemune, A. Hasegawa, K. Sakai, *Tetrahedron: Asymmetry* **1995**, *6*, 55.
- [20] Crystallographic data (excluding structure factors) for the structures reported in this paper have been deposited with the Cambridge Crystallographic Data Centre as supplementary publication no. CCDC-116486 (3), 116487 (5), 116488 (8), 116489 (9), 116490 (10), 116491 (12), 116492 (14). Copies of the data can be obtained free of charge on application to CCDC, 12 Union Road, Cambridge CB2 1EZ, UK (fax: (+44) 1223-336-033; e-mail: deposit@ccdc.cam.ac.uk).
- [21] M. G. Scaros, P. K. Yonan, S. A. Laneman, P. N. Fernando, *Tetrahedron: Asymmetry* **1997**, *8*, 1501.
- [22] For other examples of benzene inclusion complexes, see: K. Endo, T. Sawaki, M. Koyanagi, K. Kobayashi, H. Masuda, Y. Aoyama, *J. Am. Chem. Soc.* **1995**, *117*, 8341; A. Collet, *Tetrahedron* **1987**, *43*, 5725; S. Cerrini, E. Giglio, F. Mazza, N. Y. Pavel, *Acta Crystallogr. Sect. B* **1979**, *35*, 2605.

- [23] For a discussion of the effects of halogens in H-bonding, see J. A. Swift, R. Pal, J. M. McBride, *J. Am. Chem. Soc.* **1998**, *120*, 96.
- [24] For examples of H-bonding in dicarboxylic acids, see: C. B. Aakeröy, M. Nieuwenhuyzen, *J. Am. Chem. Soc.* **1994**, *116*, 10983; C. B. Aakeröy, P. B. Hitchcock, *J. Mater. Chem.* **1993**, *3*, 1129.
- [25] For examples of diastereomeric enrichment with related systems, see: a) A. Kawashima, A. Hirayama, *Chem. Lett.* **1991**, 763; **1990**, 2279; M. Kawashima, R. Hirata, *Bull. Chem. Soc. Jpn.* **1993**, *66*, 2002. See also: b) K. Tanaka, A. Moriyama, F. Toda, *J. Org. Chem.* **1997**, *62*, 1192; c) Y. Dobashi, K. Kobayashi, A. Dobashi, *Tetrahedron Lett.* **1998**, *39*, 93; d) H. Nishiyama, T. Tajima, M. Takayama, K. Itoh, *Tetrahedron: Asymmetry* **1993**, *4*, 1461.
- [26] P. H. Hünenberger, J. K. Granwehr, J.-N. Aebischer, N. Ghoneim, E. Haselbach, W. F. van Gunsteren, *J. Am. Chem. Soc.* **1997**, *119*, 7533.
- [27] See for example: D. P. Fairlie, M. L. West, A. K. Wong, *Curr. Med. Chem.* **1998**, *5*, 29.
- [28] Z.-F. Xie, H. Suemune, K. Sakai, *J. Chem. Soc. Chem. Commun.* **1987**, 838.

Received: November 30, 1998 [F1464]